Controlled human exposures to aerosol particles

Design, characterization and evaluation of aerosol generation system and chamber exposures

Christina Isaxon

Master Thesis in Environmental Engineering

Ergonomics and Aerosol Technology
Department of Design Sciences
Lund University

ISRN LUTMDN/TMAT-5118-SE
EAT 2008

Abstract

An increasing number of studies show correlations between airborne particle exposure and health problems. Since people spend most of their time (>85 %) indoors, the quality of the indoor air is of special interest. A research project has been initiated to investigate what effects indoor particles can have on our health. The project is cooperation between Ergonomics and Aerosol Technology (EAT), Lund, Division of Occupational and Environmental Medicine, Lund and Karolinska Institute, Stockholm. In the first phase of this project human test subjects are being exposed to two common indoor/industrial particle sources: candle smoke and welding fume. Both sources generate particles in the nano scale size range. Welding fume is of special health interest since these particles are strongly enriched in metal species.
The aim of this master's thesis was to develop well controlled methods for generating these particle sources and to evaluate a 22 m^3 stainless steel exposure chamber with regard to parameters such as air exchange rate, mixing of the air volume and wall deposition. Several methods were used - for the chamber evaluation: trace gas, pressure drop measurements and particle decay measurements - to confirm the results. Finally exposure data throughout the first part of the exposure series are summarized.

Representative concentrations, size distributions and chemical composition of the two exposure aerosols in homes and in industrial environment respectively were identified through literature studies and related projects (which are not part of this master's thesis) at Lund University. An aerosol generation system was then designed to meet the demands of a representative aerosol with regard to these parameters.
For the candle exposure events 6-10 candles of a common type generated a mean mass concentration of 200 $\mu g/m^3$ and a mean number concentration of 900 000 cm^{-1}. The candles were made to burn in an intermediary mode which rendered both nucleation mode particles and larger soot particles.
Welding was made in mild steel with commonly used electrode and shielding gas. Generating the fume in pulses instead of continuously gave a mean mass concentration of 1000 $\mu g/m^3$ and an exposure pattern that resembles real industrial environments. Care was taken not to exceed the health limit value of manganese, which – together with iron oxides - is a main constituent in welding fume.
The generation system's dilution and a short residence time of particles gave a relevant degree of aerosol dynamic effects, such as coagulation. The system provides real time monitoring of the concentration and ways to quickly regulate the amount of aerosol that is being delivered into the exposure chamber.
The chamber air is being thoroughly monitored with regard to number and mass concentrations, size distribution, temperature, relative humidity and carbon dioxide levels. At occasions filter samples are being collected to verify the chemical composition of the exposure aerosol.
In summary the aerosol generation method and exposure chamber were found to be a very useful system for 3-6 hour exposures of 3 human test subjects at a time.

Sammanfattning

Ett ökande antal studier har visat samband mellan exponering för luftburna partiklar och hälsoproblem. Eftersom människan spenderar största delen av sin tid (>85 %) inomhus är kvaliteten på denna luft av särskilt intresse. Ett forskningsprojekt, vars syfte är att undersöka hälsoeffekter av partiklar i inomhusluften, har startats som ett samarbete mellan Ergonomi och Aerosolteknologi (EAT), Lund, Arbets- och Miljömedicin, Lund och Karolinska Institutet, Stockholm. I projektets första fas skall frivilliga försökspersoner exponeras för två vanliga inomhus/industriaerosoler: Stearinljusrök och svetsrök. Båda dessa aerosolkällor genererar partiklar i nanometerstorlek. Svetsrök är av särskilt intresse ur hälsosynpunkt eftersom dess partiklar är starkt metallberikade.

Syftet med detta examensarbete har varit att utveckla väl kontrollerade metoder att generera dessa partiklar och att utvärdera en 22 m^3 exponeringskammare i rostfritt stål med avseende på parametrar som luftomsättningshastighet, luftomblandning och väggdeposition. Flera olika metoder har använts – för kammarutvärderingen: spårgasmätningar, tryckfallsmätningar och mätningar av partikelavklingning. Slutligen har data från den första delen av exponeringsserien summerats.

Representativa koncentrationer, storleksfördelningar och kemisk sammansättning, i hemmiljö respektive på arbetsplatser, av de två exponeringsaerosolerna identifierades med hjälp av litteraturstudier och relaterade projekt (dessa ingick inte i detta examensarbete) på Lunds Universitet. Ett aerosolgenereringssystem designades sedan utifrån dessa kriterier.

Vid stearinröksexponeringarna användes 6-10 ljus av vanlig typ, vilket under exponeringsdagen genererade en medelmasskoncentration på 200 $\mu g/m^3$ och en medelantalskoncentration på 900 000 cm^{-1}. Med hjälp av en rörlig fläkt uppnåddes en form av intermediär förbränning, då ljuslågan brann stadigt och stilla ibland och fladdrade ibland, vilket resulterade både i partiklar skapade av nukleering och större sotpartiklar.

Svetsningen utfördes på kolstål med en typ elektrod och skyddsgas som ofta används inom industrin. Svetsningen utfördes inte kontinuerligt utan i pulser, vilket resulterade i medelmasskoncentrationer på 1000 $\mu g/m^3$ och i ett exponeringsmönster som stämmer väl överens med det på en arbetsplats. En betydande del av svetsröken består av mangan och järnoxider. För mangan finns ett 8 h gränsvärde, vilket inte fick överstigas under exponeringstillfällena.

Genereringssystemets snabba utspädning och korta uppehållstid gav en acceptabel grad av åldring hos aerosolen (främst med avseende på koagulering). I systemet finns också möjlighet att i realtid övervaka koncentrationen och möjlighet att snabbt reglera mängden aerosol som transporteras till kammaren.

Luften i exponeringskammaren övervakas noggrant med avseende på antals- och masskoncentration, storleksfördelning, temperatur, relativ luftfuktighet och koldioxidhalt. Vid tillfällen har filterprover tagits för att verifiera aerosolens kemiska sammansättning.

Sammanfattningsvis har aerosolgenereringssystemet och exponeringskammaren visat sig vara mycket användbara vid 3-6 timmars exponeringar av grupper om 3 försökspersoner.

Abbrevations and symbols

A	Area
AER or a	Air Exchange Rate
b	Mobility
C_0	Concentration at time 0
C_1	Particle concentration by supplied air
C_c	Cunningham slip correction factor
C_{inc}	Concentration in incoming air
$C(t)$	Concentration at time t
CMD	Count Median Diameter
CPC	Condensation Particle Counter
D	Diffusion constant
d or d_p	Particle diameter
D_c	Characteristic particle dimension
DMA	Differential Mobility Analyzer
e	Elementary charge ($1.6 \cdot 10^{-19}$ Coulomb)
$E_{r,m}$	Mass emission factor
$E_{r,n}$	Number emission factor
EC	Elementary Carbon
F_D	Drag force
F_f	Force of friction
F_i	Force of inertia
FCAW	Flux-Cored Arc Welding
FID	Flame Ionization Detector
GC-MS	Gas Chromatography – Mass Spectrometry
GMAW	Gas Metal Arc Welding
GTAW	Gas Tungsten Arc Welding
HEPA	High Efficiency Particulate Air filter. Removes at least 99.97 % of airborne particles 0.3 μm in aerodynamic diameter, which is the most penetrating particle size (MPPS). Particles larger or smaller than this are filtered with even higher efficiency.
IC	Ion Chromatography
J	Particle flux
K	Boltzmann's constant ($1.381 \cdot 10^{-23}$ J K^{-1})
K_0	Coagulation constant
Kn	Knudsen number
LPI	Low Pressure Impactor
M_w	Molecular weight of water
MMD	Mass Median Diameter
n	Number of elementary charges on a particle
N	Number concentration
P	Pressure
p	Vapour pressure
PIXE	Particle Induced X-ray Emission

PM	Particulate Matter, e g PM2.5 indicates the total mass of particles smaller than 2.5 μm in diameter, PM10 the total mass of particles smaller than 10 μm in diameter.
p_m	Vapour pressure where tha vapour is in equilibrium with a plane surface of pure water
Ppb	Parts per billion
Ppm	Parts per million
Q	Air flow
R	Universal gas constant (8.314 J mol^{-1} K^{-1})
Re	Particle Reynolds number
RH	Relative Humidity; the ratio of the partial pressure of vapor in a system to the to the saturation vapor pressure for the whole system at the temperature of the system.
RESPI	Respiratory Particle deposition Instrument
SMAW	Shielded Metal Arc Welding
SMPS	Scanning Mobility Particle Sizer
Std dev	Standard deviation
STP	Standard Temperature and Pressure, i e 293 K and 101 kPa
T	Time
T	Temperature
TEM	Transmission Electron Microscopy
TEOM	Tapered Element Oscillating Microbalance
TSP	Total Suspended Particulate matter
ULPA	Ultra Low Penetration Air filter. Removes at least 99.999 % of airborne particles 0.12 μm or larger.
V	Relative velocity
v_d	deposition velocity
V_r	Volume
VOC	Volatile Organic Compound(s)
α	Mixing factor
β	Sum of loss mechanisms
γ	Surface tension
η	Viscosity
λ	Mean free path
ρ	Density
ρ_w	Density of water

Contents

Introductory remark

I have had the privilege to spend 15 months at EAT, of which the last 12 have been as full time employee. During this time I have dealt with several interesting tasks, of which the ones mentioned below have not been part of this master's thesis.

Together with Joakim Pagels and Anders Gudmundsson and staff from YMK and the institute IUTA, Duisburg, Germany, I have been sampling and analyzing air at three different welding workshops in Malmö and Svedala. I have constructed a Hering low pressure impactor which we used for collecting samples in the welding workshops for TEM analysis.

Designing and evaluating the generation system have been a part of the work for my master's degree, while conducting the actual exposure events have been part of my employment here. I have, together with Joakim Pagels, been responsible for the aerosol generation at the exposure events and for the measurement instruments related to the exposures. I have been evaluating data from the exposure events as well as from the field measurements in the welding workshops and presented these data and methods used to obtain it at a METALUND seminar in Lund, at the European Aerosol Conference in Thessalonike, Greece and at Inhaled Particle X in Sheffield, UK. I have also been first author of the abstracts submitted to these two conferences (Isaxon et al. 2008a, 2008b).

I have been developing and evaluating a method to generate particles from ozone-terpene reactions that is being used in the next phase of the exposure project. I have also had a part of the practical responsibility considering the exposures, such as making the scedule and recruiting human test subjects.

Furthermore I have been coordinator for a course given by EAT at Malmö högskola called "Innemiljö", been contact person for the students and lecturers, handled the laboratory practical, corrected labreports and assisted in correcting exams.

Together with Anders Gudmundsson I have rigged, installed and later dismantled an indoor measurement station that has been used to monitor indoor air in a residential home.

I have been assisiting Joakim Pagels and Aneta Wierzbicka in their studies of indoor aerosol sources (Pagels et al. 2008).

1. Introduction

An increasing number of studies show correlation between exposure to airborne particles and health problems. Since humans, at least in the industrialized parts of the world, tend to spend the major part of their life indoors (>85 %), particles in these environments are of special interest. As the development of new measurement instruments is progressing, the understanding for which particle properties affect our health is increasing, and more extensive studies of aerosols and their health influence are motivated and needed.

An aerosol is defined as particles (in solid or liquid phase) suspended in a gas, normally air. Aerosols are hence (at least) two-phase systems, and they include a wide range of phenomena such as dust, fume, mist, fog, haze, clouds and smoke (Hinds, 1999). Every cubic centimeter of the air that surrounds us normally contains thousands of particles,of many origins: for example suspended soil particles, smoke from industrial activities such as welding, photochemically formed particles, salt particles from ocean spray, atmospheric clouds of water droplets or ice particles and particles generated from our daily activities such as burning candles, doing the laundry or cooking. Particle sizes range from about 0.002 μm to more than 100 μm (Hinds, 1999), the lower limit defined by particles so small that they only consist of a few molecules and the upper limit by the size where the particles are too big to remain in suspension. Particles that have one dimension less than 100 nm are referred to as *ultra fine particles* or *nano particles*, particles that are smaller than 1 μm as *fine particles* and those larger than 1 μm as *coarse particles* (Hinds, 1999). In "clean" air the particle concentration can be less than 1000 particles per cm^3, while it can easily exceed 10^6 particles per cm^3 in industrial environments.

Indoor particles may penetrate a building from outdoor air or may be emitted directly from indoor sources (Lai & Nazaroff, 2000). Major indoor sources in home environment are tobacco smoking, cleaning, cooking, and candle- and incense burning (Hussein et al, 2006). In industrial environments fine and ultrafine particles of significantly higher concentrations occur compared to home indoor environments, and they are often enriched in health relevant chemical species, for example metal oxides (Jenkins & Eagar, 2005). One especially interesting aerosol when it comes to investigate health effects is welding fume (Isaxon et al, 2008a,b), since the fume is strongly enriched in metal and since the welding industry is extensive – the total amount of smoke emitted from welding processes yearly is estimated to 5000 tons (Redding, 2002)

Therefore, the division of Ergonomics and Aerosol technology (EAT), Lund, has, together with the Karolinska Institute (KI), Stockholm, and Occupational and Environmental medicine (AMM), Lund, initiated a research program to investigate the health impact of particles emitted from typical indoor sources, such as candles and occupational exposure to welding fume. The specific aims of the research program are to perform well-controlled experimental studies on the direct measurable physiological effects on humans exposed to these sources. The particles are well characterized with respect to particle concentration (number, surface area and mass), chemical composition, solubility and hygroscopicity. The exposure effects that will be investigated are general symptoms, lung function, heart rate variability, coagulation and inflammatory markers in the mucous membranes (see Appendix C for a more detailed description of these medical

examinations). The human test subjects are healthy adults, and will be exposed three at a time. Each group of test subjects will be exposed twice – at one occasion for particles and at another for clean filtered air. The exposures are double blind, so that neither the subjects nor the medical staff will know whether or not the subjects have been exposed to elevated particle concentrations at that particular time. The exposure levels will represent realistic scenarios in normal indoor/workplace environments on the occasions when these sources are active.

2. Objective

The general purpose of this master thesis is to develop methods that can be used to gain better understanding of potential health effects induced by particle inhalation at concentrations relevant to real-life indoor and occupational situations. For this purpose a method which utilizes exposure studies in a well controlled chamber environment are being executed in a project involving the division of Ergonomics and Aerosol Technology (EAT), Occupational and Environmental medicine (AMM) and the Karolinska Institute (KI). In the first phase of this project, adverse effects of candle smoke and welding fume particles are being investigated. The stainless steel exposure chamber is located at Ingvar Kamprads Designcenter (IKDC), Lund University, Faculty of Engineering.

The specific objectives of this master thesis are to develop the particle generation and chamber for the human exposure studies, in terms of:

- a literature study of welding fume aerosol characteristics,
- evaluation of the exposure chamber with regards to parameters such as air exchange rate, mixing of air volume and wall deposition,
- theoretical design and practical construction of an aerosol generating system for candle and welding fume particles,
- evaluation of the generating system during the first phase of the exposure study.

3. Background and Theory

3.1 Aerosol physics relevant for particle formation, chamber exposures and aerosol measurement

To be able to foresee and retrieve knowledge of health risks connected to the inhalation of particles, one must know how particles are formed, transported and deposited.
To understand aerosols is to understand the interactions between particles (solid or liquid) and the suspending gas, thus it is necessary to comprehend certain features of the gas itself, such as mean free path, viscosity and diffusivity.
When it comes to describing the particle/gas interaction a key feature is the Reynolds number, which governs whether a flow is laminar or turbulent. The Reynolds number is included in the Stoke's law, required for understanding particle motion. Important concepts are also the different equivalent diameters.

3.1.1 Aerosol formation and growth

Aerosol formation can be caused either by natural occurring processes (for example erosion, sea spray or volcanic activity) or by anthropogenic sources.
One significant formation process is conversion of vapor and/or gases to particles. This occurs for example during combustion processes, when the high temperatures result in very high vapor pressures so the majority of the fuel and reaction products are present in the vapor phase. During the cooling process the vapor becomes super saturated. If the saturation is high enough, at least several hundred percent, very small (a few nanometers) particles can be formed. This process is termed nucleation. The process of nucleation can be divided into four different types:
a) Homogenous homomolecular nucleation, where gas molecules of the same chemical composition unites to form a particle.
b) Homogenous heteromolecular nucleation, where gas molecules of two or more different chemical compositions unites to form a particle.
c) Heterogeneous homomolecular nucleation, where gas molecules of one chemical composition adhere to already existing particles of another chemical composition.
d) Heterogeneous heteromolecular nucleation, where gas molecules of several chemical composition sticks to already existing particles of another chemical composition (Akselsson, 1994).

Particle formation can also be caused by chemical reactions between different gases under the influence of UV radiation (Akselsson et al, 1994).

Condensation of water is governed by the relative humidity of the surrounding air. Relative humidity is defined as the ratio of the partial pressure of vapor in a system to the saturation vapor pressure for the system at a given temperature. The saturation vapor pressure is the amount of water vapor that (at the pressure and temperature in question) is in equilibrium with a plane surface of pure water.

Water vapor in equilibrium with water in aerosol particles has a somewhat different vapor pressure due to the curvature of the surface and to the solved salts (salts obstruct the evaporation from the particles, which shifts the equilibrium towards lower vapor pressure).

The curvature of a particle causes the surface molecules to be more loosely bound to their neighbor molecules than they would have been if the surface was flat, hence it takes a higher vapor pressure to achieve equilibrium. This effect of the particle curvature is called the *Kelvin effect* and can be formulated as

$$\frac{p}{p_m} = e^{\frac{4\gamma M_w}{\rho_w RTd}} \tag{3.1}$$

where γ is the surface tension, M_w the molecular weight of water, ρ_w the density of water and d the diameter of the droplet. P_m is the vapor pressure where the vapor is in equilibrium with a plane surface of pure water.

High-temperature aerosols (such as for example welding fume) are subjects to a very strong temperature gradient. The higher the temperature the easier it is for a chemical specie to remain in gas phase, but a combustion aerosol is quickly cooled off which results in a strong super saturation that in turn leads to nucleation and a quick particle growth due to condensation. The saturation ratio caused by the temperature gradient is much larger than the saturation ratio resulting from the Kelvin effect, meaning that for high temperature aerosols the Kelvin effect is relevant when it comes to the process of nucleation only (small particles give a large Kelvin ratio). Also, during a high-temperature process, a specie can be chemically transformed into another (such as the transformation of sulphur dioxide to sulphate) which has a much lower vapor pressure, thus increasing the saturation ratio by several orders of magnitude.

3.1.2 The motion of particles in a gas

Three kinds of forces can act upon an aerosol particle and affect its motion: external forces, friction forces (air resistance) and forces between particles (attractive and repellant). Particle motion is caused primarily by external forces, such as gravity or forces from an electric field, and resistance forces from the surrounding gas. The relation between the force that pushes away the surrounding gas (force of inertia), F_i, and the friction force (viscous force), F_f, between the particle and the gas is defined as the particle Reynolds number:

$$Re = \frac{F_i}{F_f} = \frac{\rho V D_c}{\eta} \tag{3.2}$$

where ρ is the density of the gas, V is the relative velocity between the gas and the

particle, D_c is a characteristic dimension for the particle (for example diameter) and η is the viscosity of the gas (the viscosity of air at 293 K is $1.81 \cdot 10^{-5}$ Pa·s). The Reynold's number hence characterizes fluid flow around an obstacle, such as an aerosol particle[1].

At a low Reynolds number the inertial forces are negligible compared to viscous forces, and here *Stoke's law* applies:

$$F_D = 3\pi\eta V d_p \tag{3.3}$$

Most aerosol motion occurs at low Reynolds numbers (Re<1) because of the low velocities and the small particle sizes involved, hence Stoke's law is applicable to most aerosol-motion related problems.
An important assumption in Stoke's law is that the relative velocity of the gas right at the surface of the particle is zero. For small particles, whose size approaches the mean free path (see Appendix A) of the gas, this assumption is not correct. To account for this the *Cunningham slip correction factor*, C_c, is introduced (Aerosoler, 1994):

$$C_c = 1 + Kn(1.257 + 0.400e^{-1.1/Kn}) \tag{3.4}$$

where *Kn* is the Knudsen number, defined as $2\lambda/d_p$, where λ is the mean free path for a molecule of the gas and d_p is particle diameter.
The slip correction factor is always bigger than one and reduces the drag force in Stoke's law by

$$F_D = \frac{3\pi\eta V d_p}{C_c} \tag{3.5}$$

Slip correction increases as pressure decreases because of the dependence of mean free path through the Knudsen number. When a particle has a diameter significantly smaller than the mean free path of the molecules in the surrounding gas (at STP this corresponds to d_p<0.02 μm), it is said to be in the *free-molecule region*. Here the air counteracts the particle's motion as a series of discrete impacts. When d_p>3 μm the surrounding gas affects the particle as a continuum, this region is called the *continuum region*. The region between these two is named the *transition region*. The Cunningham slip correction factor corrects Stoke's law so that it can be used for particle motion in all these regions.

The ratio V/F_D is called *mobility*, *b*. According to eqn (1.5), *b* is:

$$b = \frac{C_n}{3\pi\eta\, d_p} \tag{3.6}$$

[1] The bigger the object the higher the Reynolds number, for example a sperm cell has Reynold's number of $1 \cdot 10^{-2}$ while a blue whale has one of $3 \cdot 10^{8}$.

Mobility and driving force determine the stationary velocity of a particle. Gravity as driving force for example leads to sedimentation, collisions due to the thermal motion lead to diffusion (Burtscher, 2005). The mobility is directly related to the diffusion constant *D* by the stokes-Einstein relation (3.9):

$$D = b \cdot kT \tag{3.7}$$

3.1.3 Deposition mechanisms

Deposition describes the processes that remove particles from an aerosol through adhesion on macroscopic surfaces, for example losses to the walls in indoor environments, or the deposition of particles in the respiratory tract. Deposition mechanisms are also what make it possible to sample air with impactors or collect particles on various filters. The most important deposition mechanisms are diffusion, sedimentation, impaction, interception, electrical forces and thermophoresis.
Deposition is often given as a *deposition rate* value, in units of h^{-1} and defined as the number of particles deposited on the total surface available per unit of time divided by the total number of particles in the air.

3.1.3.1 Diffusion

Diffusion is the motion of gas molecules driven by a concentration gradient (from an area with higher concentration to an area with lower concentration). Due to van der Waal forces[2], aerosol particles adhere when they collide with a surface, thus inducing a zero aerosol concentration just above that surface. As a result a concentration gradient is established in the region near the surface causing a continuous diffusion of particles to this surface, as diffusion is driven by differences in concentration. This results in a gradual decay in concentration with time. The flux (quantity transferred per unit time through a unit area perpendicular to the direction of diffusion) is given by *Fick's law*:

$$J = -D\frac{dC}{dx} \tag{3.8}$$

D is the diffusion coefficient, or the diffusivity. The diffusivity for air at standard conditions is $2.0 \cdot 10^{-5}$ m^2/s.
The diffusivity's relation to particle diameter (d_p) is given by the *Stokes-Einstein equation*:

$$D = \frac{kT\,C_c}{3\pi\eta\,d_p} \tag{3.9}$$

[2] The van der Waal force is an attraction force of electrical nature. It is strong but has a very short range of operation and is caused by the temporary electrical dipoles that emerge due to continuous variations in the electron configuration in all materials.

which explains why diffusion has a big significance for small particles (less than 0.1 μm), whilst other deposition mechanisms dominate for larger particles.

3.1.3.2 Sedimentation

When a particle is released in air, it quickly reaches its terminal settling velocity, which is a condition of constant velocity wherein the drag force of the air on the particle is exactly equal in size and opposite in direction to the force of gravity. Terminal settling velocity is proportional to the square of the particle diameter, so it increases rapidly with particle size.
Mobility is the ratio of the terminal velocity of a particle to the steady gravitational force producing that velocity. It has units of m/(N·s) and is often called mechanical mobility to distinguish it from electrical mobility (Hinds, 1999).

3.1.3.3 Impaction

Impaction occurs when a particle due to its inertia can not follow the streamlines of the air and due to this adheres to a surface. The larger the particle and the higher the velocity, the bigger the possibility is of impaction.

3.1.3.4 Interception

A particle that has an amount of inertia small enough to follow the air's streamlines can be deposited through interception. This occurs when a streamline carrying a particle passes the surface closer than the particle radius. The possibility for interception naturally increases with particle size. It is mostly important in the size range where other deposition mechanisms are weak, between 0.1 and 1 μm. It is a deposition mechanism especially important for fibers.

3.1.3.5 Electrical Forces

A particle can be charged the moment it is formed or it can be charged by collisions with ions from the surrounding air. If the air contains ions of both positive and negative charge the aerosol will eventually achieve a bipolar equilibrium charge distribution. This is because a charged particle surrounded by ions of both polarities will attract ions of the opposite polarity and repell ions of the same polarity. Due to their small size the ions have a much higher diffusivity than the aerosol particles and will hence collide with and stick to aerosol particles. This diffusion will eventually lead to neutralization of the aerosol. This, however, does not imply that every particle will have zero charge. The equilibrium charge distribution can be approximately described by the Boltzmann distribution, which states the probability for a particle to carry *n* elementary charges.

Most particles 0.1 μm or larger carry some small net charge which induces an equal and opposite charge in the surface (Hinds, 1999). The electrostatic adhesion force is proportional to the first power of the particle diameter (Hinds, 1999).

An aerosol particle in an electrical field, carrying *n* charges, experiences an electrical force causing it to move through the gas in which it is suspended. When the force from

the electric field is in equilibrium with the resistance force from the gas, it quickly reaches its terminal velocity. The resulting drag force on the particle can be equated to the electrical force to determine the electrical mobility, Z_p, of a particle. In other words, the electrical mobility is a measure of the particle's ability to move in an electric field, and is defined by:

$$Z_p = \frac{neC_c}{3\pi\mu d_p} \tag{3.10}$$

where:

n = number of elementary charges on the particle
e = the elementary charge ($1.6 \cdot 10^{-19}$ Coulomb)
C_c = Cunningham slip correction factor
μ = gas viscosity
d_p = particle diameter

3.1.3.6 Thermophoresis

A temperature gradient in the gas surrounding a particle will induce a net force making the particle move towards areas with lower temperature. This transport is due to the fact that gas molecules in the warmer areas will transfer a bigger amount of momentum to the particle than molecules in the colder areas (Akselsson, 1994). Thermophoresis is a deposition mechanism relatively non dependent of particle size and is an important mechanism in combustion processes and when sampling high temperature aerosols, because of the strong temperature gradients.

3.1.4 Coagulation

Coagulation is a term that describes how particles collide with and stick to each other, hence decreasing the number concentration of the aerosol and increasing the particle size. *Brownian coagulation* is a type of coagulation that is spontaneous and always present in an aerosol, induced by the Brownian motion of the particles. Assuming monodisperse spherical particles with diameter exceeding 100 nm the rate of change in the number concentration due to this coagulation can be described as (Hinds 1999):

$$\frac{dN}{dt} = -K_0 N^2 \tag{3.11}$$

where K_0, the coagulation coefficient, is dependent on the diffusion coefficient, D, and on the first power of the particle diameter as:

$$K_0 = 4\pi d_p D \tag{3.12}$$

Because the rate dependency of the second power of the number concentration, coagulation is rapid at high concentrations but slows with time as the number of particles is reduced. To know the net effect of coagulation over some period of time, t, equation (xx) is integrated over this period and solved for N(t), resulting in:

$$N(t) = \frac{N_0}{1+N_0 K_0 t} \tag{3.13}$$

As a rule of thumb, coagulation is neglected in laboratory experiments and occupational hygiene works if the concentration is less than 10^6 cm^{-3} (Hinds, 1999). If a generated aerosol has a concentration higher than this the coagulation process can be stopped by rapid dilution with particle free air to concentrations below the one stated above. However, in certain types of experiments, when precision requirements are high and time scales are long (for example when studying slow processes such as wall deposition in indoor environments), coagulation can have a measurable effect down to concentrations of 10^3 cm^{-3}.

3.1.5 Aerosol particle diameter

Particle size is the most important parameter for predicting the behavior of an aerosol. Most aerosols cover a wide spectrum of sizes; a hundredfold range between the smallest and largest particles of a given aerosol is common (Hinds, 1999). Since a particle often is more or less irregular in shape it is not straight forward to define its diameter, hence an *equivalent diameter* is often used. This term refers to the diameter of the sphere that has the same value of a particular physical property (often related to a measurable property) as that of the particle in question. The diameter of a spherical particle may be determined

by optical or electron microscopy, by light scattering and Mie[3] theory, by its electrical mobility or by its aerodynamic (e. g. inertial) behavior. Thorough insight to the different equivalent diameters is particularly important when interpreting measurements on highly irregular particle shapes as those commonly found from high temperature processes, such as welding, and soot particles. Some of the most useful equivalent diameters are listed below:

Aerodynamic diameter: The diameter of the spherical particle with density 1000 kg/m^3 that has the same settling velocity as the particle in question. The aerodynamic diameter can hence be thought of as the diameter of a water droplet having the same aerodynamic properties as the particle (Hinds, 1999). This diameter is important for transport, collection and respiratory tract deposition of larger particles.

Volume equivalent diameter is defined as the diameter of a sphere that has the same volume as the actual particle. To determine the volume equivalent diameter takes thorough knowledge of the particle which is not easily observed by measurement, and this equivalent diameter is not as frequently used as the aerodynamic equivalent diameter.

Mobility equivalent diameter (also called *Stokes diameter*) is the diameter of a sphere having the same mobility as the particle under consideration.

With enough knowledge of the particle it is possible to transform one type of equivalent diameter into another, which is of value when results from different measurement instruments are to be compared.

3.1.6 Respiratory tract deposition

The most relevant mechanisms for deposition in the respiratory system are impaction, sedimentation and diffusion. The respiratory system can be divided into three main regions: the *head airways* (from nose/mouth to larynx), the *tracheobronchials* (from larynx to the terminal bronchioles) and the *alveols*. In the head airways the main deposition mechanism is impaction. If a person breathes through the nose the most deposition occurs there, while a person who breaths through the mouth will have the main deposition at the larynx. For particles with a diameter less than 100 nm diffusion can be a significant deposition mechanism in this region, increasing in significance if the particle diameter is even smaller. The head airways do not have cilium and it is most probably the pharyngeal lymphatic ring, located in the pharynx, which deals with our defense against foreign matter deposited in this region.

For particles bigger than 2-3 µm impaction in the tracheobronchial region is the dominant mechanism, for particles between 0.5 and 2 µm sedimentation dominates (sedimentation is favored by small horizontal parts of the airways where the air velocity is low and the

[3] Mie scattering is the predominant scattering process for particle sizes larger than the wavelength of the incoming light. The process, which is not very wavelength dependent, produces for example the almost white glare around the sun when a lot of particulate material is present in the air, and also the white light from mist and fog.

vertical distance to the wall is small). For particles smaller than 100 nm, diffusion is of importance also in this respiratory region. All of the tracheobroncial region (except for parts of the larynx) is coated with cilium. These flicker in a coordinated manner with a frequency of 10-20 times per second transporting mucous, and in that deposited particles, upwards to the larynx. It takes deposited particles approximately 0.5, 2 and 5 hours to be transported by this mechanism from the broad, medium broad and fine airways respectively.

In the lowermost airways (alveolar region) there is very little mixture between just inhaled air and residual air (air that remains since previous breaths). The deposition of particles between 100 nm and 1 µm in this region is governed by the transfer of particles from the newly inhaled air to the residual air. Almost all the particles will be deposited once transferred – the smaller particles through diffusion and the larger through sedimentation. The mechanisms for particle transportation from the alveolar region are not completely known, but can occur by devouring of the particle by phagocytes.

Really small particles will not reach the alveolar region as their high diffusion rate will make them deposit before they reach this far down the respiratory system (Akselsson et al, 1994). In summary the nose is an effective pre-filter for particles larger than a couple of µm, which makes the human lungs fairly well protected from coarse particles, while fine and ultra fine particles will have a large potential to penetrate and deposit in the more vulnerable lower respiratory tract. Figure 3.1 shows the regional deposition as a function of particle size according to the ICRP Task Group Lung Model.

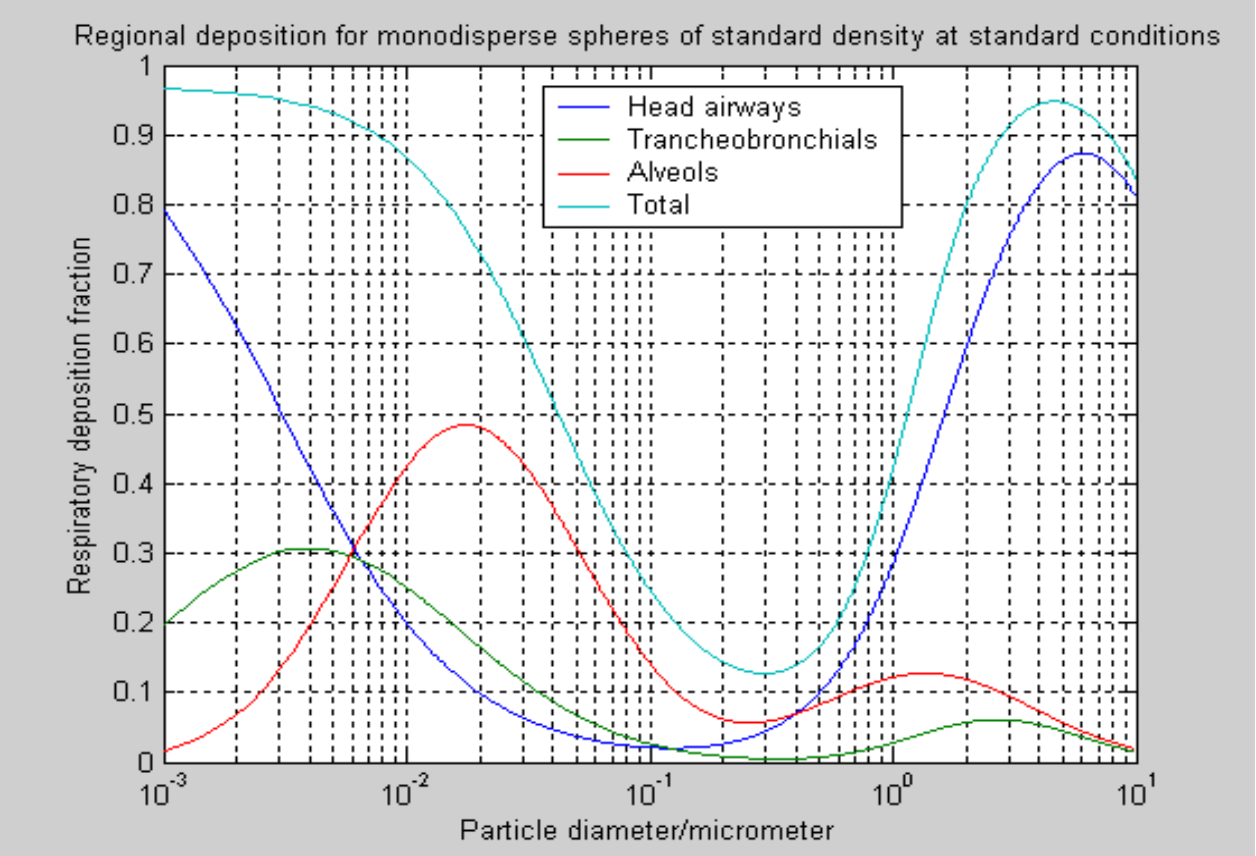

Figure 3.1. Fraction of deposition in the respiratory system according to the ICRP model (figure by Pontus Roldin). At the right hand of the minimum at 200-400 nm the main deposition mechanisms are impaction and interception and on the left hand diffusion.

3.2 Theory and background to aerosol chambers and aerosol generation

3.2.1 Aerosol chambers

One of the advantages of using an exposure chamber when investigating health effects of inhaled particles is that the chamber provides a well controlled environment. Volume, air flow, aerosol mass- and number concentration, temperature and relative humidity are just some of the parameters that are possible to monitor and control. Ichitsubo et al. (2003), when developing a radon-aerosol exposure chamber, concluded that chamber temperature and relative humidity have very little effect on particle concentration and their size distributions, nevertheless control of these parameters are of course of importance for the human test subjects.

When an aerosol enters the chamber several different things can happen to it depending on particle size and chemical composition. The particles can be deposited to the walls and floor by some of the previously mentioned mechanisms and also, depending on its concentration, undergo higher or lower degrees of coagulation. The magnitude of these

effects in the chamber depends to a large extent on the time the aerosol resides there. The air exchange rate (AER) is a characterization of the efficiency of the ventilation system. AER is often given in the unit h^{-1} thus providing a measurement of how many times per hour 63 % (1-1/*e*) of the air volume in a room is exchanged under the presumption that the mixing between the incoming air and the air in the chamber is complete.

3.2.2 Aerosol Generation System

Achieving a well controlled aerosol with high demands of specific particle size distribution as well as chemical composition, requires a well planned generation system. It needs to be designed considering facts such as reproducibility, residence time, and dilution. It also has to be possible to regulate the amount of generated aerosol let into the dilution system and further on into the exposure chamber and the system needs to be flexible to allow generation of as many different types of aerosols as possible. The human test subjects in the exposure chamber should preferably not be able to notice whether an aerosol is transferred into the chamber at a particular time or not, hence the generation system should not be visible for test subjects or medical staff, nor should it be very noisy.

McDonald et al. (2006) designed a wood smoke generation and exposure system using a conventional stove and a controllable dilution system. They generated well characterized combustion aerosols of different mass concentrations intended for exposure studies.

A relevant concentration of the aerosol used in the exposure studies has to be determined. This is made with regards taken to relevant concentrations on work/indoor environments and threshold limit values for health relevant species, foremost manganese in welding fume (100 $\mu g/m^3$). The aim is to expose the test subjects to “normal” concentrations of the aerosol in question. Extensive field studies were made for determining what “normal” levels are, these studies are outside the frames for this master thesis, but are briefly reviewed below (and in more detail in Appendix B).

3.2.3 Aerosol sources

Both welding and candle particles are aerosols formed in high temperature processes involving steep temperature gradients. An aerosol formed in high temperature is quickly cooled off leading to a strong super saturation which results in a quick particle formation and subsequent growth due to condensation. The saturation can be further increased due to chemical transformations into species with lower vapour pressure, which can occur in these temperatures.

3.2.3.1 Candle smoke particles

In several field studies in home environments, candles have been identified as sources of ultrafine particles, larger accumulation-mode particles and a major contributor to indoor elemental carbon (EC) and PM2.5 concentrations (Pagels et al, 2008). Wierzbicka et al (2008) have preformed field measurements to determine what particle concentrations different activities in the home can result in. As seen in figure 3.2 candle burning results

in a significantly high number concentration compared to many other particle generating activities.

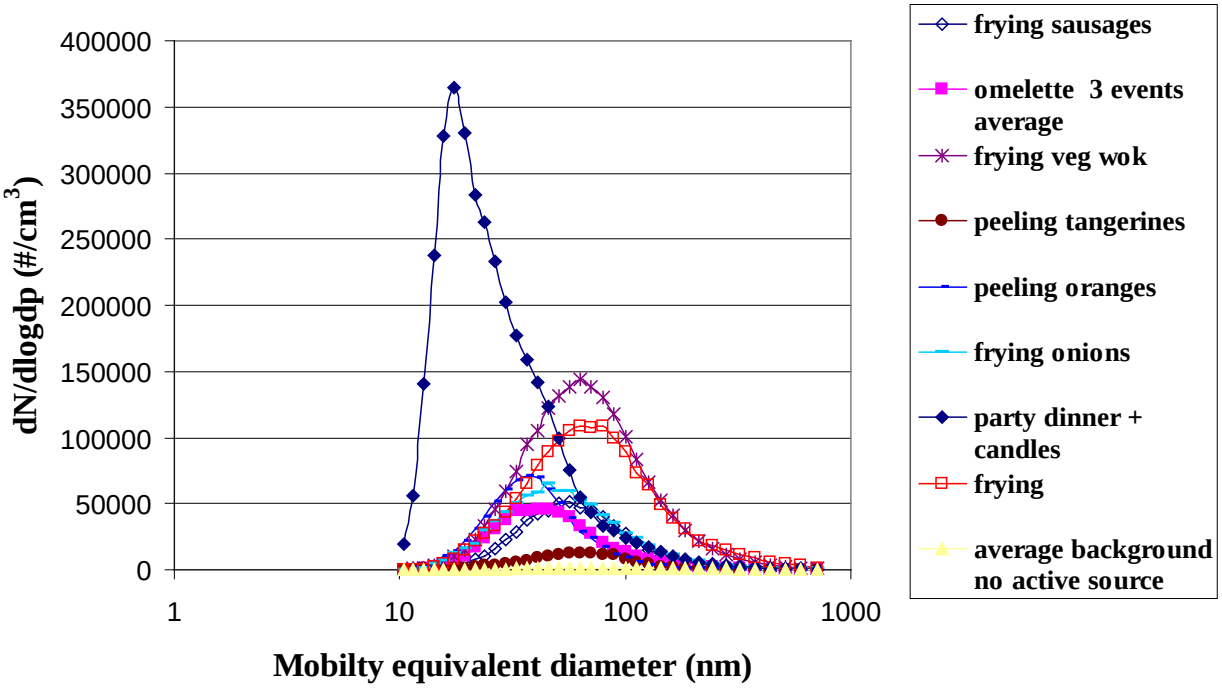

Figure 3.2. Number size distributions of particles generated by various indoor activities (Wierzbicka, 2008)

A candle is made of a solid wax material - mainly stearin, which is a product containing carbon, hydrogen and a carboxylic acid - the top of which melts to produce a pool of liquid that soaks into the wick. With help of capillary forces the wick serves as a transport for the fuel to the flame itself. Although solid at room temperature, pure stearin liquefies at about 150 ^{o}C and then becomes gaseous; a process which is associated with decomposition into lighter species. The chemical reactions involve not only oxygen and the fuel species, but also reaction products, atoms and radicals: O, OH, CH_3, HCHO etc (Borghi, 1998) ; the slightly blue color that is observable at the base of the flame is the emission of visible light by the CH radical. The chemical reactions form CO_2 and water vapor and increase the temperature of the medium. The combustion process also forms soot, which are particles of slightly hydrogenated carbon. The soot particle oxidation is visible in the flame due to the yellow light emitted. During steady laminar burn in principle all soot is oxidized in the flame. This type of steady burn forms ultra fine primary particles with an average diameter around 20 nm, mainly consisting of phosphates or alkali nitrates. Air movements in the vicinity of the flame, caused by for example people moving around in the room or an open window, may result in soot particles being able to escape without being oxidized, thus resulting in EC emissions (Pagels, 2008). This mode of burning is referred to as “sooting combustion” and the particles are highly agglomerated and have a diameter of about 250 nm (figure 3.3). A third burning mode is “smouldering”, which refers to the white smoke produced upon extinction of a candle. The particles formed in this process are rich in organics and have a

mean diameter of 300 nm. Pagels et al. also reported mass emission factors during the different modes of burning.

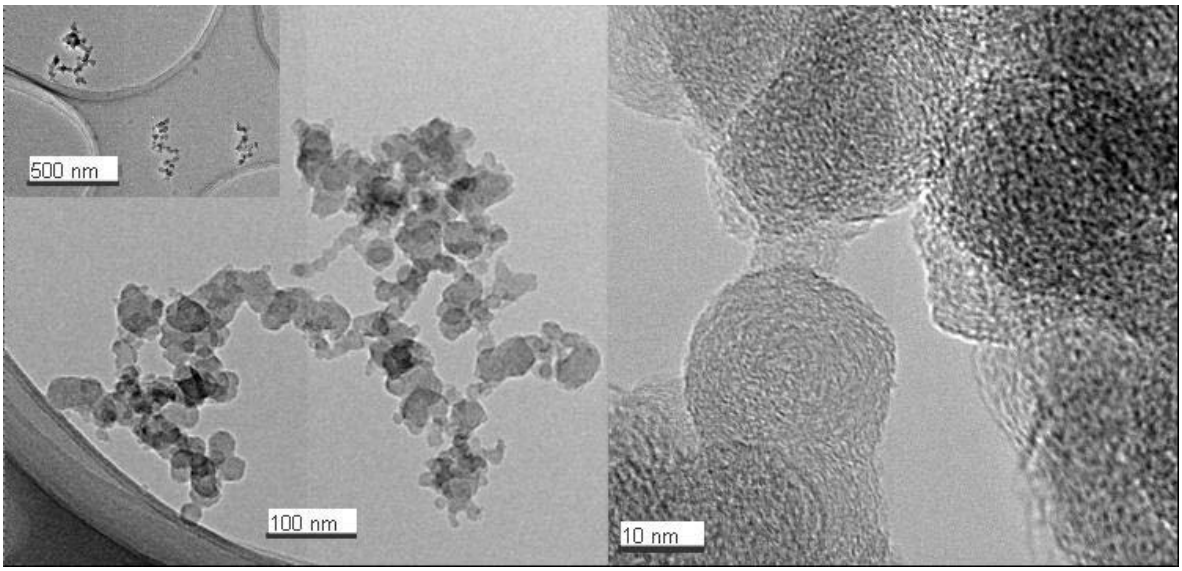

Figure 3.3. TEM images of particles in the soot mode at different magnification (Pagels et al. 2008)

3.2.3.2 Welding fume particles

To obtain detailed characterization of welding workshop aerosols, studies were made at three different workshops in and around the Malmö area. Samples were taken at two different points, in the background air and directly in the welding plume at each of the workshops (See appendix for a more detailed description of methods and instruments employed in this field study).

The results from these studies together with an extensive literature study on welding fume were later on used to select exposure levels in the chamber and control that the laboratory generated welding fume was representative.

The formation and characteristics of welding particles are reviewed in the literature study below.

3.2.4 Literature study on welding fume characteristics

The art of joining metals dates as far back as the Bronze Age, and in present time a large amount of welding methods have been developed. The major part of the methods uses an electrically generated arc to melt an electrode that drips down on the workpieces, forming a pool of molten material (the weld pool). The welding region is sometimes protected by some sort of inert or semi-inert gas, known as a shielding gas. When the weld pool cools a strong joint is formed.

Among the most common industrial methods are SMAW (*Shielded Metal Arc Welding*), GMAW (*Gas Metal Arc Welding*), FCAW (*Flux-Cored Arc Welding*) and GTAW (*Gas Tungsten Arc Welding*). SMAW is also known as manual metal arc welding or stick welding. In this process the consumable electron rod is covered with a flux that protects the weld area from oxidation and contamination by producing CO_2 during the welding process (Wikipedia, search word: welding). FCAW resembles GMAW but uses a wire consisting of a steel electrode surrounding a powder fill material. This type of wire is more expensive but permits higher welding speed and deeper metal penetration. GTAW, also called TIG (*Tungsten Inert Gas*), is a fully manual process that uses a non consumable tungsten electrode, a shielding gas and a separate filler material (Antonini, 2003). The method requires significant operator skill but renders high quality results.

The GMAW process uses automatized and continuous electrode wire feed and an inert or active shielding gas, and is the method that is used for the exposure experiments. It is one of the most frequently used indoor welding methods. The electrode and the shielding gas are both fed through a nozzle, see figure 3.4. Typical electrode feeding speeds are 2 to 10 m/min. The GMAW welding method is often referred to as MIG (*Metal Inert Gas*) or MAG (*Metal Active Gas*) depending on the composition of the shielding gas; when it contains CO_2 it is termed active. Inert types of shielding gas are for example argon and helium. The shielding gas protects the molten metal from oxidation, which would lead to pore formation, by simply creating a microclimate around the welding point, shielding it from the oxygen and nitrogen in the surrounding air. The method is not well suited for outdoor situations since the constant movement of the outdoor air disturbs the flow of the shielding gas. The electric arc is, with the help of a power supply, maintained between the electrode and the base material. Commonly the electrode is negatively charged and the base material positive, resulting in a deeper penetration and a higher welding speed than had the charges been the other way around (T. Bratz, 2007). The composition of the electrode is mainly determined by the composition of the substrate, since the aim is a welding joint with mechanical properties similar to the substrate's. Other than iron, a GMAW electrode normally contains some metal like aluminum, manganese, titan or silicon, which has the purpose of protecting the welding material from oxidation. The choice of shielding gas also depends on the substrate; inert gases are only used when welding non-ferrous substrates. A welding process is often optimized by using a mixture of inert and active gases.

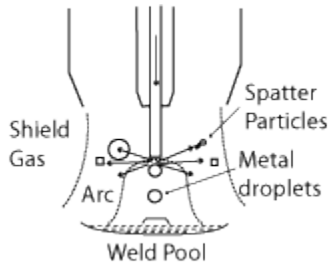

Figure 3.4. Schematic picture of the GMAW-process (after Zimmer et al. 2002).

The total amount of smoke emitted from the welding industry is estimated to 5000 tons/year (Redding 2002), of which a non-negligible part ends up in the welders' lungs. Epidemiological studies show that many welders suffer from lung problems (Antonini et al. 2006). Kalliomaki et al (1983) studied shipyard mild steel (< 0.15 % carbon) arc welders and found the net rate of alveolar deposition of iron in full time welders to be 70 mg per year. After 10 years of welding, the average burden of ferrous metal particles in the lung was 1 g. Retired welders were found to clear 10-20 % of the accumulated particle mass per year. Welders are of course not a homogenous group, making the negative health effects of welding difficult to evaluate. Also the industrial buildings are different, so are the welding methods, materials, ventilation and other workshop activities (which can generate for example solvents, asbestos or silicon). In the forging industry a worker combines welding with other activities, but in the shipbuilding or wind mill industry a worker could weld more or less continuously for seven, eight hours a day.

The welder works bent over the welding substrate, close enough to clearly see the welding pool. A helmet is used, mainly for protecting the eyes and face from the UV light. Some welders use more advanced helmets in which a slight overpressure is sustained to prevent fume particles from entering. Studies have been conducted by Goller and Paik (1985) to compare the iron oxide fume concentration inside and outside of the helmet which resulted in a measured reduction of fume concentrations in the actual breathing zone inside the mask to 36 – 71 % of the concentrations outside the helmet, depending on the welding process and posture of the welder (Antonini, 2003). An extractor hood is often available at the work station, but this is far from always used.

3.2.4.1 Fume generation

The droplets from the electrode can be transferred to the metal welding substrate by two different methods: globular droplet transfer or spray droplet transfer. Spray transfer GMAW is the most common method (and it is also the method that we will use in the human exposure studies).

Arc welding causes about 10 % of the consumable welding electrode to vaporize. Most of the vapor recondenses in the weld pool, but approximately one tenth of it travels out of the high-temperature arc region and condenses into metal oxide nanoparticles that aggregate into submicron clusters (Jenkins, 1997). In aerosol research the term *fume* is used to describe air-borne metal or metal oxide particles condensated from vapor phase.

The term fume also includes bigger particles created by ejection of droplets. These particles, called *spatter*, are often too big to be air-borne since their diameter often exceeds 20 μm. If it does not, they are called *microspatter* or *sputter*.

Spray droplet transfer is associated with high applied currents and has the following characteristics: a conical arc that surrounds the column of irregularly shaped/sized metal droplets, high electrical resistance with a calculated mean droplet temperature of ~2750 ^{o}C, enhanced transfer of metal vapors resulting in high fume formation rates (FFR) (Zimmer et al. 2002). For GMAW, the fume formation rate varies between 0.035 and 0.37 g/min (Zimmer and Biswas, 2001) and depends on what current and what voltage is being used (Quimby and Ulrich, 1999). The current is regulated by the welder and is a determined by the composition and thickness of the substrate (T. Bratz, 2007). The shielding gas typically runs at a flow of 25 lpm and a normal electrode feed speed is 1.25 mm/s. A fume formation rate of 10 mg fume per gram of wire is common, which is equivalent to saying that 1 % of the wire evaporates (Jenkins, 2003).

More and smaller particles are formed with spray droplet transfer than with globular droplet transfer (Jenkins et al, 2005). Measurements made by Zimmer et al. (2002) showed that spray droplet transfer generated one order of magnitude more particles smaller than 16.5 nm than globular droplet transfer did. This is most probably due to the the fact that the alloy droplets generated by spray droplet transfer has a bigger surface- to volume ratio.

Since fume from GMAW mainly consists of particles smaller than 1 μm a large part of the fume is respirable (Jenkins et al, 2005).
The fume density from GMAW is 5-6 g/cm^3 (Jenkins, 2003).
Not only the wire but also the shield gas composition affects the fume formation rate and its size distribution, see figure 3.5.

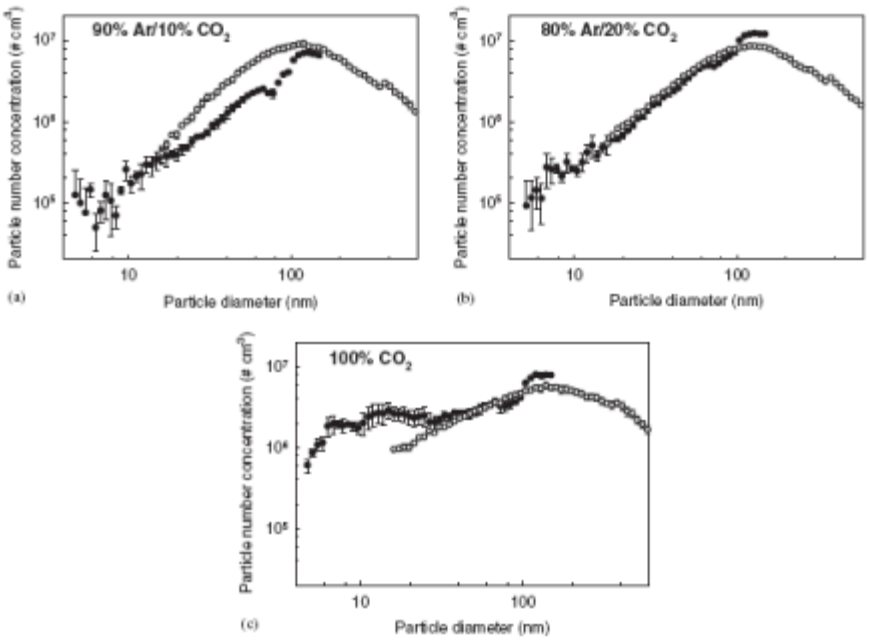

Figure 3.5. SMPS results for GMAW: (a) using a 90 % Ar/10 % CO_2 shield gas, (b) 80 % Ar/ 20 % CO_2 shield gas and (c) 100 % CO_2 shield gas. The measurements were made at the same height 19.2 cm above the arc centerline using both a nano DMA (dark circles, 4.53 nm < d_p < 153 nm) and a long DMA (hollow circles, 16.5 nm < d_p < 562 nm). When 100 % CO_2 is used the nucleation mode is clearly visible (Zimmer et al. 2002).

Pure CO_2 increases the fume formation rate by a factor 2.7 compared to a shield gas composition of 93 % Ar 5 % CO_2 2 % O_2 (Zimmer at al. 2002). The reason for this is that CO_2 can work as a source of oxygen at the high temperatures present and will then contribute to the evaporation from the spray droplets (Redding C. J. 2002).

Spray droplet transfer will generate very little spatter, almost negligible compared to globular droplet transfer (MIG/MAG Welding Guide, 1997). The fume from spray-GMAW contains less than 6 mass percent micro spatter (Jenkins et al. 2005), all of it being in the sub micrometer range (Zimmer & Biswas, 2001). This difference in fume rate between the two operating modes can be explained by considering how the arc works at the two operating modes. The purpose of the arc is to detach metal droplets from the electrode so that these can end up at the substrate and contribute to the formation of the welding joint (the joint consists of molten electrode and molten substrate). During globular transfer the arc is held constant at the tip of the electrode whose surface heats up and electrode metal evaporates to diffuse into the gas stream where it later oxidizes and condensates to form fume. When a droplet detaches from the electrode, the area of the neck decreases to a point where enormous heat is released because of the rising resistance and high current. This generates metal vapors at explosive rates, ejecting micro-droplets into the gas phase. Thus, under globular transfer, both evaporation and explosive detachment contribute to the fume.

In spray mode, the arc is no longer focused at the bottom of the growing drop but moves around detaching droplets and up the side of the melting electrode, so explosive ejection is no longer a major contributor to fume (Quimby & Ulrich, 1999).

Directly above the arc the particle mass concentration is 100-400 mg/m^3. The concentration in the breathing zone varies depending on which welding method is being employed, but levels of 5 mg/m^3 are typical throughout the industry (Zimmer & Biswas, 2001).

3.2.4.2 Formation mechanisms and chemical composition

Most of the materials in the welding fume come from the electrode; a small fraction of the fume is derived from spatter and from the molten welding pool. The shielding gases, base material or surface coatings also contribute some to the composition of the welding aerosol. With the help of ICP-AES (*Inductively coupled Plasma-Atomic Emission Spectrometry*) researchers have found that the welding fume is reasonably independent of the welding substrate and that almost all of the species found in the fume can be derived from the electrode material (Antonini et al, 2006). The substrate only seems to influence the fume composition if it is covered with oil, paint or any other similar substance (Quimby & Ulrich, 1999). These assumptions are logical considering the fact that the temperature at the tip of the electrode (approx 3100 K) is higher than that of the weld pool at the substrate (Jenkins et al., 2005). Components of the aerosol can be modified, either thermochemically in the welding zone, or by photochemical processes driven by ultraviolet light emitted during welding. Vaporized metals react with air, producing metal oxides that condense and form fume consisting of particles that are mainly of respirable size (Antonini, 2003).

The dominating aerosol formation mechanisms during GMAW are nucleation, where metal fume at high temperatures devolves to primary particles (0.01-0.10 μm) followed by growth through coagulation. The chemical properties of welding fumes can be quite complex. Different pure metals commonly found in the materials used in welding evaporate at different rates at a particular elevated temperature depending on the vapor pressures (Antonini, 2003). In his doctoral thesis, Jenkins concluded that primary particles formed from the same well mixed fume shows compositional variation that depend on primary particle size, see table 3.1.

Table 3.1. Atomic fraction of metals content in mild steel gas metal arc welding fume per size group. Manganese mole fraction of the electrode was 0.012 (Jenkins, 2003).

	20 nm	Std	40 nm	Std	60 nm	Std	80 nm	Std	Bulk Fume
Fe	0.881	0.050	0.901	0.050	0.933	0.037	0.888	0.147	0.89
Mn	0.119	0.050	0.099	0.050	0.067	0.037	0.112	0.147	0.11

In the GMAW process the molten metal in the end of the electrode emits steam that mixes with the shield gas and then travels through a 10-20 mm wide zone at speeds of 100 m/s, from the arc temperature of well above 3000 K (boiling point of iron) to room temperature. This means that steam and particles reside in the hot zone for about 10^{-4} s and are exposed to a temperature gradient of 10^{7} K/s. Particles nucleate, grows and are blown out of the hot vapor rich areas where they cease growing. The size of the particle at this point is determined by a combination of the critical diameter of nucleation and the rate of condensation. For this reason, the primary particle size becomes an indication of the temperature at which the particle was formed and this temperature, in turn, is an indicator of the elementary composition of the condensed particle. At about 80 nm this variation in composition vanishes and the particle composition is the same as the fume composition. It can therefore be reasonable to assume that particles of that size has not been formed by one single nucleus, but rather by collision and merging of more than one primary particle, which could even out the composition variations within the particle. At the coagulation that follows, agglomerates are formed through particle-particle collisions, particle-agglomerate collisions and agglomerate-agglomerate collisions. The agglomeration is enhanced by the turbulent condition that is a result from heat generated during the welding process, thus increasing particle movement and chances for particle collision (Antonini, 2003). The agglomerates have a chain-like structure (Jenkins & Eagar, 2005; Zimmer & Biswas, 2001; Antonini et al, 2006) as shown in figure 3.6 below. The primary particles are mainly formed from magnetite (γFe_3O_4), which due to the magnetism of the compound forms the chains.

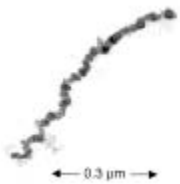

Figure 3.6. TEM photo of a GMAW generated aerosol particle (Zimmer & Biswas, 2001). The particle consists of homogenous chain-like aggregates.

One can expect to find manganese in the oxidation states Mn^{2+} and Mn^{3+} and ferrous oxides such as FeO, Fe_2O_3 and Fe_3O_4 in the welding fume. If the particle is larger than half a micron it can consist of several phases, normally with a nucleus of high iron content. Particles smaller than this will not be constituted of more than one phase since they, due to their small volume, will be homogenized very quickly (Jenkins, 2003; Jenkins & Eagar, 2005).

Since the size range of welding particles is so big - four orders of magnitude from 0.005 to 20 µm – it is very complicated to analyze the chemical composition using only one method. One way to deal with this is to separate the fume into different size groups with the use of a cascade impactor, for example <0.1 µm, 0.1-0.5 µm, 0.5-1 µm and >1 µm (Jenkins & Eagar, 2005). The first group will then contain particles that are small enough

to be deposited in the alveoli region, and the last group (>1 μm) will contain the particles that are deposited in the nose and throat, rendering a size separation that will facilitate inhalation-toxicological analysis. The analysis method is then chosen from the size range of interest.

The aerodynamic mass median diameter of the agglomerates were by Antonini 2006 measured to be 0.24 μm and by Zimmer & Biswas (2001) to 0.149 μm; sizes that have a high prevalence of being deposited in the alveolar region.

The agglomerates are held together by magnetic forces (Zimmer et al. 2002) and electrostatic and van der Waal forces (Antonini et al, 2006). The magnitude of these forces is of toxicologic relevance since interaction with the lung tissue and biological fluids can break the bonds in the agglomerates and make the primary particles dissociate. This causes the surface area of the aerosol to increase and hence the toxicity. It is not possible, however, to analyze overall toxicity based on the individual toxicities of the respective components of the fume. While two chemicals may be non toxic when ingested alone, they may prove fatal when ingested together or vice versa (Jenkins doctoral thesis).

3.2.4.3 Temporal variations in number concentration

The arc welding aerosol is similar to a combustion aerosol and will be significantly altered depending on where it is sampled (Zimmer & Biswas, 2001). Figure 3.7 shows a TEM-image of welding fume:

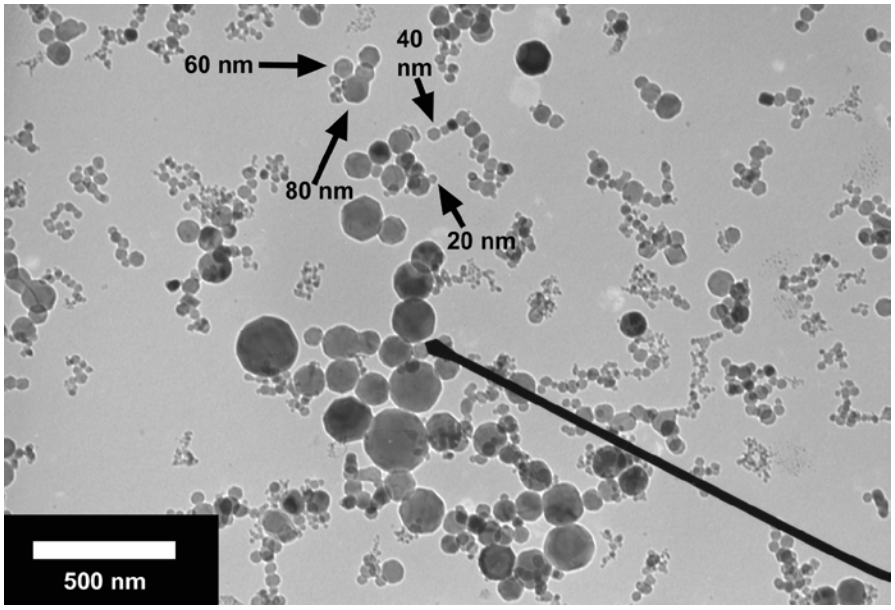

Figure 3.7. GMAW-generated welding fume (Jenkins 2003).

Zimmer & Biswas (2001) noted that the number concentration decreases four-fold from a distance of 4.8 cm to a distance of 19.2 cm from the welding nozzle, and that the concentration varies more the closer to the nozzle the sampling point is located. This fluctuation is assumed to be due to the high temperature in combination with the shielding gas, which will create instability and local turbulence. The decrease in concentration with sampling height should mainly be attributed to the dilution of the fume by the surrounding air and to coagulation of the fume particles. Another fact noted during this experiment was that the average number concentration actually increased with time on distances further away from the arc; at a point 19.2 cm vertically and 15 cm horizontally from the welding nozzle the concentration increased from $3.2 \cdot 10^6$ cm^{-3} during the measurement period 25-75 s to $5.1 \cdot 10^6$ cm^{-3} during the period 175-225 s (figure 3.8). A explanation could be that the welding process heated the substrate resulting in a buoyant thermal plume that increased the dispersion of the welding fume, resulting in a slight increase in concentration. During the whole measurement period a temperature increase from 21 ^oC to 264 ^oC just above the surface of the substrate was noted.

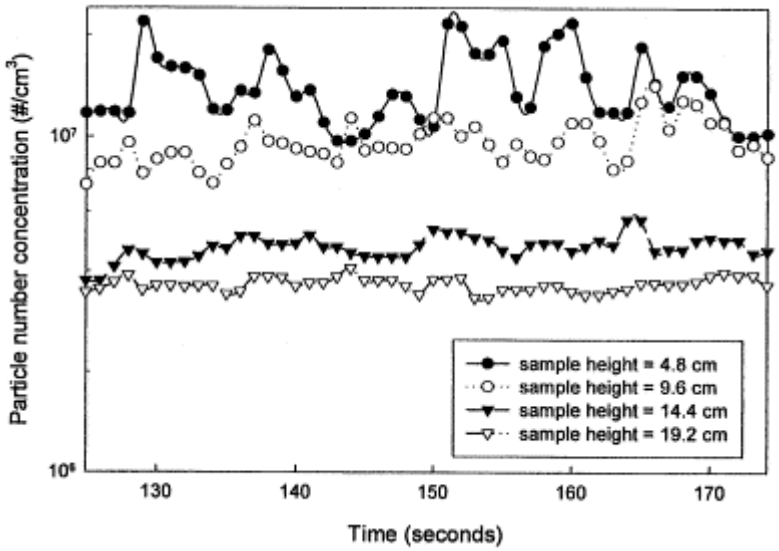

Figure 3.8. CPC results for a 50 s period with measurements taken horizontally along the arc centerline.

In a following experiment Zimmer & Biswas (2001) added filtered air to dilute the fume 150 times and measured the number concentration at three sample heights corresponding to increasing residence times (figure 3.9). It was clear that the number concentration for the smaller particles decrease substantially when residence time is increased, for example the number concentration of particles smaller than 40 nm decreased with a factor of 20 between sampling height 4.8 cm to 19.2 cm. The reason for this is that these small particles are scavenged by larger ones through coagulation.

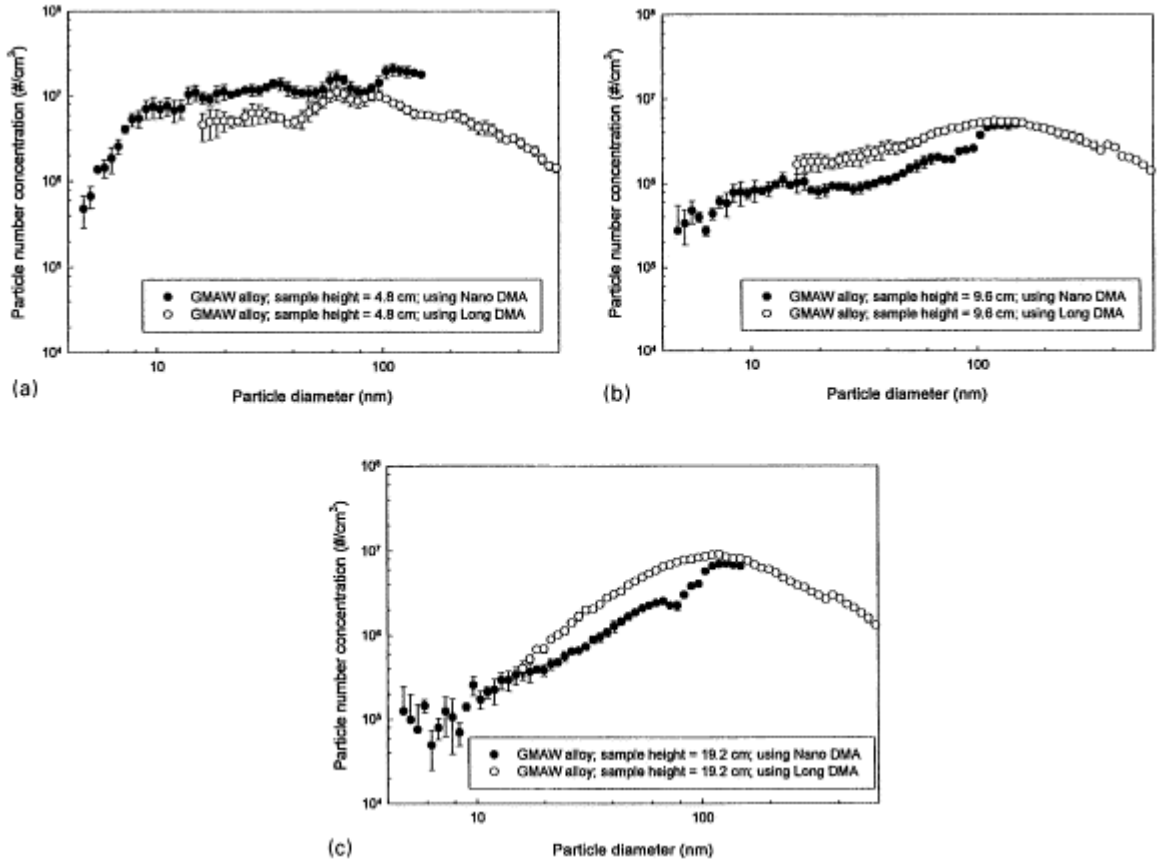

Figure 3.9. SMPS results for a GMAW alloy: (a) 4.8 cm, (b) 9.6 cm and (c) 19.2 cm above the arc centerline using both a nano DMA (4.53 nm < d_p < 153 nm) and a long DMA (16.5 nm < d_p < 562 nm), (Zimmer & Biswas, 2001).

The differences noted could be related to the physical differences between the DMAs, in that the geometry of the nano DMA was optimized to minimize diffusion losses while the long DMA was designed to characterize particles over a broad size range.

3.2.4.4 Gases formed during welding

Several toxic gases, such as carbon monoxide, ozone and oxides of nitrogen, may be generated in significant amounts during welding. These gases have different origins depending on welding process, includig shielding gases, decomposition products of electrode coatings and cores, reaction in the arc with atmospheric constituents, reaction of ultraviolet light with atmospheric gases and decomposition of degreasing agents or coatings on the metal substrate (Antonini, 2003). The most important gases generated are:

Ozone
During welding ozone is formed from a photochemical reaction between atmospheric oxygen and the ultraviolet radiation emitted by the arc, according to:

1. O_2 + light < 210 nm → 2O
2. O + O_2 → O_3

The formation rate of ozone is depending on the wavelengths and the intensity of the light generated in the arc, which in turn is affected by the welding substrate, the electrode type, the shielding gas, the welding process and variables such as voltage, current and arc length. Ozone is instable in air and its decomposition is accelerated by metal oxide fumes. Therefore, significant amounts of ozone are not associated with welding processes that generate large quantities of fume (such as FCAW, as opposed to GMAW) (Antonini, 2003).

Antonioni et al (2006) generated welding fume with mass concentrations of 90 – 150 mg/m^3 (compared to measured background levels of 3 – 5 $\mu g/m^3$ at Kockums welding workshop) and detected ozone at levels of 0.041±0.019 ppm. It can be noted that ”normal” background levels are around 0.025 ppm and that the threshold limit value from NIOSH (*National Institute for Safety and Health*) is 0.1 ppm. Exposure levels above 0.3 ppm can cause extreme discomfort and exposure to 10 ppm for several hours can cause pulmonary edema (Antonini, 2003).

Nitrogen Oxides
In welding processes nitrogen oxides are formed by oxidation of atmospheric nitrogen at temperatures above 1200 ^oC according to

$N_2 + O_2 \rightarrow 2NO$

The rate of formation increases with temperature. After dilution with air, NO can form nitrogen oxide:

$2NO + O_2 \rightarrow 2NO_2$

Exposure to high levels of nitrogen oxides can cause pulmonary irritation and edema. In FCAW nitrogen oxide concentrations in the welding area can be as high as 7 ppm (Howden et al, 1988, Antonini, 2003). However, at this occasion, the levels were as low as 2 ppm inside the weldes’s eye protection mask which shows that the mask *does* offer some protection other than against light.

Carbon monoxide
CO is often encountered during welding of steel when the electrode coating contain calcium carbonate or with the GMAW process when the shielding gas is CO_2 or argon/CO_2 mixtures. At the high temperatures that prevail in the arc or at the molten metal surface, CO_2 is reduced to the more chemically stable CO (Antonini, 2003).

Inhaled CO decreases the ability of the blood to carry oxygen to various parts of the body. It has been showed that concentrations of CO near the welding plume were over eight times higher during indoor welding compared to outdoor welding, but during the previous mentioned experiment (Antonini, 2003) no levels notably higher than the background levels were obtained.

3.2.5 Summary of field studies in three welding workshops

The PM10 measurements in the background zone at the three investigated workshops ranged from < 100 µg/m^3 during longer breaks, up to 3000 µg/m^3 during intense work periods (figure 3.10). Personal exposures measured as respirable dust (0.1 – 10 µm) ranged from 600-3400 µg/m^3. From the in-plume measurements the signature number size distributions from welding could be determined and typically yielded a single mode with geometric mean diameter of 100-150 nm.
The signature mass size distributions of MAG-welding also appeared as a single mode with mass median aerodynamic diameter (MMAD) of 200-300 nm, as can be seen in figure 3.11.

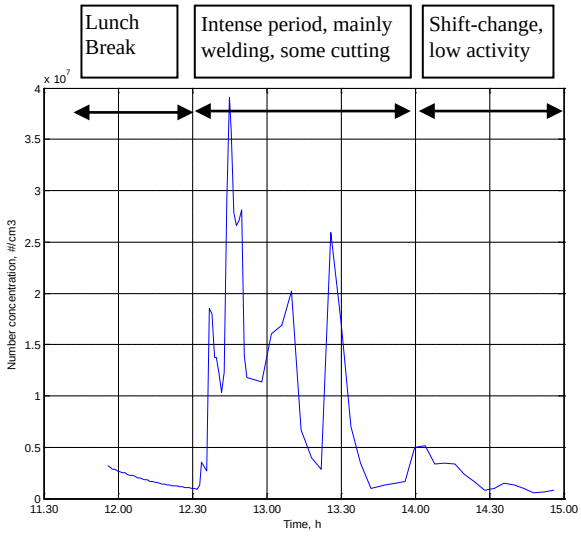

*Figure 3.10***.** Number concentrations at a background measurement point during the afternoon at a welding workshop (SMPS) (Isaxon et al, 2008).

Using PIXE analysis (described in section 4.1.4) it could be determined that the in-plume measurements of MAG-welding in mild steel have a particle composition dominated by iron (70-80 %), while the manganese fraction increases with size (from 4 to 20 % of detected elements). Further, the fraction of nickel and chromium is very low (<0.6 %), as expected for welding in mild steel (Isaxon et al. 2008).

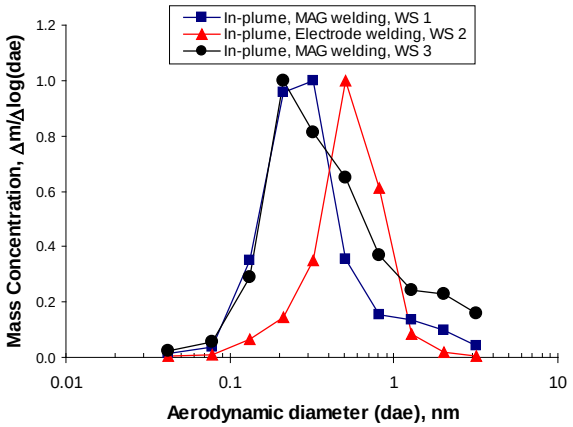

Figure3.11. Normalized mass size distributions based on elements detected with PIXE from in-plume measurements in the three workshops (Isaxon et al. 2008).

4. Methods

4.1 Laboratory work

4.1.1 The Exposure Chamber

The chamber is a 21.6 m^3 room where all interior surfaces (except for a window 0.8 m^2) are covered with a layer of stainless steel. No air can enter or leave the chamber except through a well controlled ventilation system (figure 4.1).

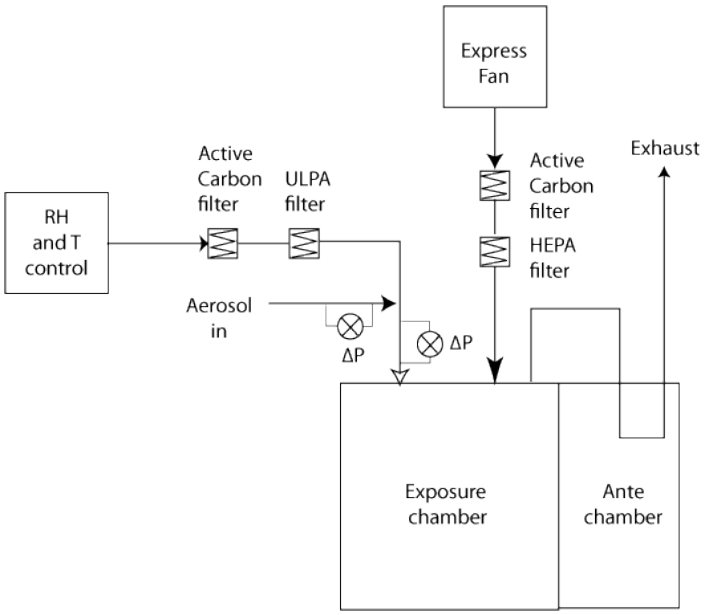

Figure 4.1. Schematic view of the chamber and its ventilation system.

The only way to enter the room is via an antechamber (3.1 m^3) with air tight doors, both to the chamber and to the surrounding laboratory. The air supplied to the antechamber is exhaust air from the chamber itself, to minimize contamination of the chamber air when entering or leaving the chamber. The chamber is supplied with air through a separate conditioning system which takes air from the room surrounding the chamber. The air flow, temperature and RH can thus be controlled and adjusted. In this work we used two different flow-settings of the supply air system, i. e. the system can be run with either one of its internal fans (fan setting "1") or both (fan setting "2"). The air passes through an activated carbon filter and an ULPA filter before entering the chamber at roof level. An aerosol containing flow can be pre-mixed with the supply air and passed into the clean air stream just above the chamber inlet. The air supply opening into the chamber is 250 mm in diameter. Two variable iris modules (*Coval, M 10*) are used to determine the clean and the aerosol-laden flow rates through pressure drop measurements. The clean supply air can, if desired, be redirected to pass through either of two lines consisting of two rotameters and a control valve, figure 4.3, before entering the filter system. Both the iris,

the flow settings of the conditioning unit and the redirection possibility provide a wide range of possible air flow values.

The chamber air exit is situated at 0.8 m height in the diagonally opposite corner of the air inlet. The exhaust flow is controlled using a variable exhaust fan. This fan is also used for achieving a desired over-pressure inside the chamber, to make sure no particles from the surrounding air will accidently enter. This pressure difference between the chamber and the surrounding room is determined and monitored using a u-tube. The over-pressure in the chamber is typically set to 10 Pa or just below. Inside the chamber there is a possibility to use a mobile rotating fan to quickly achieve complete mixing, preferentially when low air exchange rates are being employed.

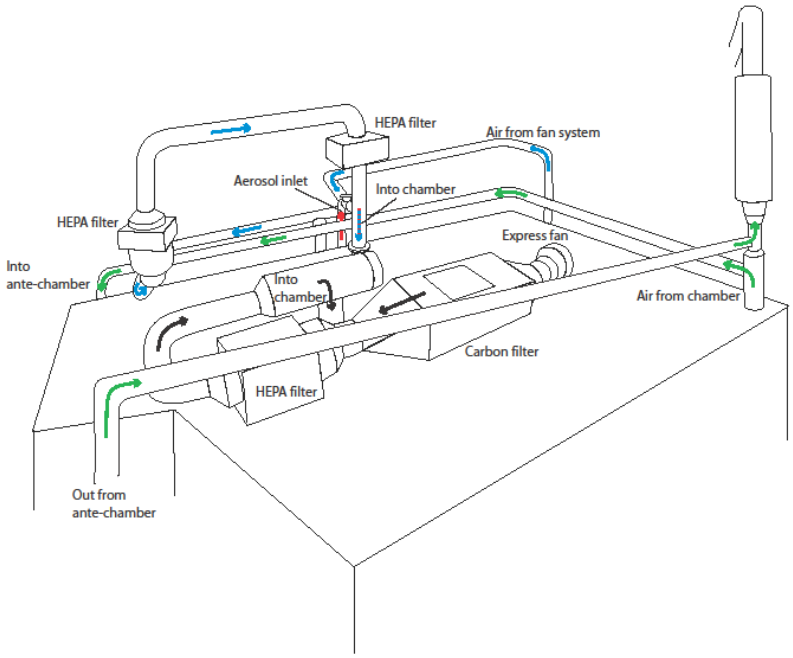

Figure 4.2. The chamber air supply system. Blue arrows denote supply air originating from the conditioning unit. Green arrows denote exhaust air originating from the chamber. Red arrow denotes generated aerosol and black arrows denote air flow generated by the express fan.

The chamber can quickly be emptied of remaining aerosols after an experiment with the help of an express fan. Then air is supplied from the surrounding room, passed through a filter with pelleted active carbon and through a HEPA filter before entering the chamber at high flow rate. The express system provides an air exchange rate (AER) of ~15 h^{-1}, and in 15-20 min the particle concentration is down to 1 % of the initial concentration. It was also looked at whether an air purifier would contribute significantly enough to make this time even shorter by evaluating results from several articles on this subject. It could be concluded that since the express fan is as effective as it is, an air purifier would not contribute significantly to the particle removal (see Appendix D).

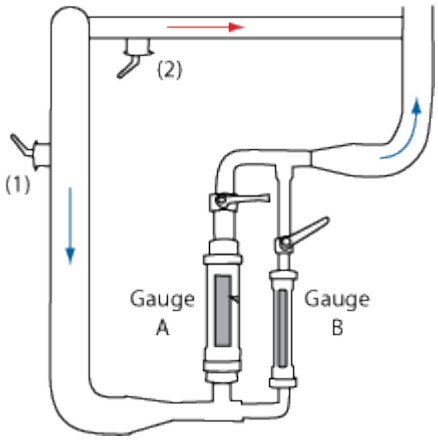

Figure 4.3. Alternative way of the chamber air flow.The red arrow denotes the original way of the air flow, just before reaching the activated carbon filter. If (2) is closed and (1) is opened the air will instead pass gauge 1 or gauge 2 before entering the filters. This provides a possibility to achieve lower air exchange rates.

The chamber can be used for human exposure as well as for source characterization and aerosol transformation studies.

A series of experiments were set up for determination of the air exchange rate and the degree of complete mixing in the chamber. Three different approaches were used to determine the AER. 1) a reference method based on trace gas measurements, 2) a method based on air flow measurements and finally 3) a method based on the decay of particle concentrations. The aim was to validate methods 2 and 3 using the more elaborate reference method. The determined AER value could then be used to determine the deposition rate to the surfaces in the chamber. These measurements were performed for several different flow settings using the conditioning unit and the express fan.

4.1.1.1 Calculations of AER using trace gas

The air exchange rate can be calculated by releasing a pulse of an inert gas (in this case SF_6[4]) in the chamber and then monitor the concentration decay. The gas was released for approximately 10 sec manually inside the chamber, in the center of the air volume. A 1312 Photoacoustic Multi-gas Monitor together with a 1303 Multipoint Sampler and Doser (*Innova AirTech Instruments*) were used for simultaneously monitor the SF_6 concentration decay in three different sampling points inside the chamber: (1) close to the diluted aerosol/clean air inlet, (2) by the wall opposite the inlet, approximately 1 m above floor level and (3) by the chamber air outlet in the upper corner furthest away from the aerosol inlet. The detection limit of the instrument is 0.009 ppm (Wierzbicka et al. 2008).

[4] Sulphur hexafluoride, SF_6, is a colourless, odourless, non-toxic gas of high chemical stability and inertness. It is also non-flammable and about 5 times as heavy as air. SF_6 is is a strong greenhouse gas with about 23 000 times the global warming potential of CO_2. Due to its stability it has a very long atmospheric lifetime (Environment Agency, 2007).

The concentration's dependence on time can be derived using a mass balance over the factors that affect the aerosol concentration in the chamber (Gustavsson, 2004):

In + Produced = Accumulated - Losses - Out

meaning:

$$QC_1 + E_{r,n} = V_R \frac{dC}{dt} - \nu_d AC - \alpha QC \tag{4.1}$$

where

C_1 = Particle concentration in supply air [#/m^3]
$E_{r,n}$ = Number emission factor [h^{-1}]
α = Mixing factor, complete mixing given by α=1
Q = Air flow through chamber [m^3/h]
ν_d = Deposition velocity [m/h]
A = Chamber area [m^2]
V_r = Chamber volym [m^3]
t = Tid [h]

(4.1) is satisfied by

$$C(t) = C_0 e^{-\frac{\alpha Q + \nu_d A}{V_r} t} + \frac{QC_1 + E_{r,n}}{\alpha Q + \nu_d A}\left(1 - e^{-\frac{\alpha Q + \nu_d A}{V_r} t}\right) \tag{4.2}$$

where
$C(t)$ = Concentration at time t [#/m^3]
C_0 = Concentration at time 0, i e initial concentration [#/m^3]

By introducing an aerosol into the chamber and, at time t = 0, shut off its generation (*ii*) is simplified to equation (4.3)

$$C(t) = C_0 e^{-\frac{\alpha Q + \nu_d A}{V_r} t} \tag{4.3}$$

By taking the logarithm of both sides of the formula a linear relation is obtained:

$$\ln \frac{C(t)}{C_0} = -\frac{\alpha Q + \nu_d A}{V_R} \cdot t \tag{4.4}$$

where the factor $\frac{\alpha Q + \nu_d A}{V_R}$ is the coefficient of slope of the straight line.

An inert gas will not deposit on the chamber surfaces and therefore ν_d in the factor $\frac{\alpha Q + \nu_d A}{V_R}$ can be set to zero with absolute certainty, and assuming complete mixing of the chamber air volume, all observed concentration decay emanate from chamber ventilation, resulting in that the straight line's coefficient of slope will be equal to the air exchange rate.

4.1.1.2 Calculations of AER using pressure drop over an iris

An iris[5] is placed on the air/aerosol pipe just before the chamber inlet (see figure 4.1). The iris can be adjusted to quench the air flow in various grades. By measuring the pressure drop over the iris (ΔP) the following relationship, provided by the iris manufacturer, can be used to obtain the air flow Q [l/s]:

$$q_v = k\sqrt{\Delta P} \tag{4.5}$$

where *g* varies with the iris setting. Since the chamber volume is known (21.6 m^3) the flow is easily transformed to air exchange rate.

4.1.1.3 Calculations of AER and wall losses from particle concentration data

Using a nebulizer, particles of NaCl (5 vol-% solution in distilled water) were introduced to the chamber. The RH was 40 % and both fans in the ventilation system were operating, which gives the highest flow that can be obtained without using the express fan. When a number concentration of approximately 100 000 cm^{-3} was achieved the generation was turned off, and using a SMPS-system the concentration decay was monitored until the levels were analogous to those in normal indoor air; 2000 – 5000 cm^{-3}.

Since particles in the size range of 200 nm have a very low probability to diffuse or sediment to the walls with the high air flow settings used, relation (4.4), with the term ν_d assumed to be 0, can be used (for high AER). If complete mixing of the air volume inside the chamber can be assumed, (α = 1), the coefficient of slope is reduced to be equal to the air exchange rate (Q/V_R).

To calculate the wall deposition the trace gas determined air exchange rate value was used. To favour deposition the AER was kept at a minimum by using only one of the two fans in the ventilation system and setting the exhaust fan to its minimal value, 1.5. The air flow is directed through rotameter B and regulated so the gauge shows a value of 5 units. The mobile fan inside the chamber is set to 70.

[5] An iris is an in-line device used to measure flow rates through pipes, by observing the pressure drop created by making the opening of the iris smaller.

Simultaneously as the trace gas decay was measured in the three points to determine the AER, the wall deposition was examined using NaCl particles dispersed from a 5 vol-% solution. The aerosol was generated in a pre-chamber, diluted with clean air (HEPA filter) to a concentration of approx 14 000 cm^{-3} and then released into the chamber air inlet.

4.1.2 Aerosol generation system for human exposure

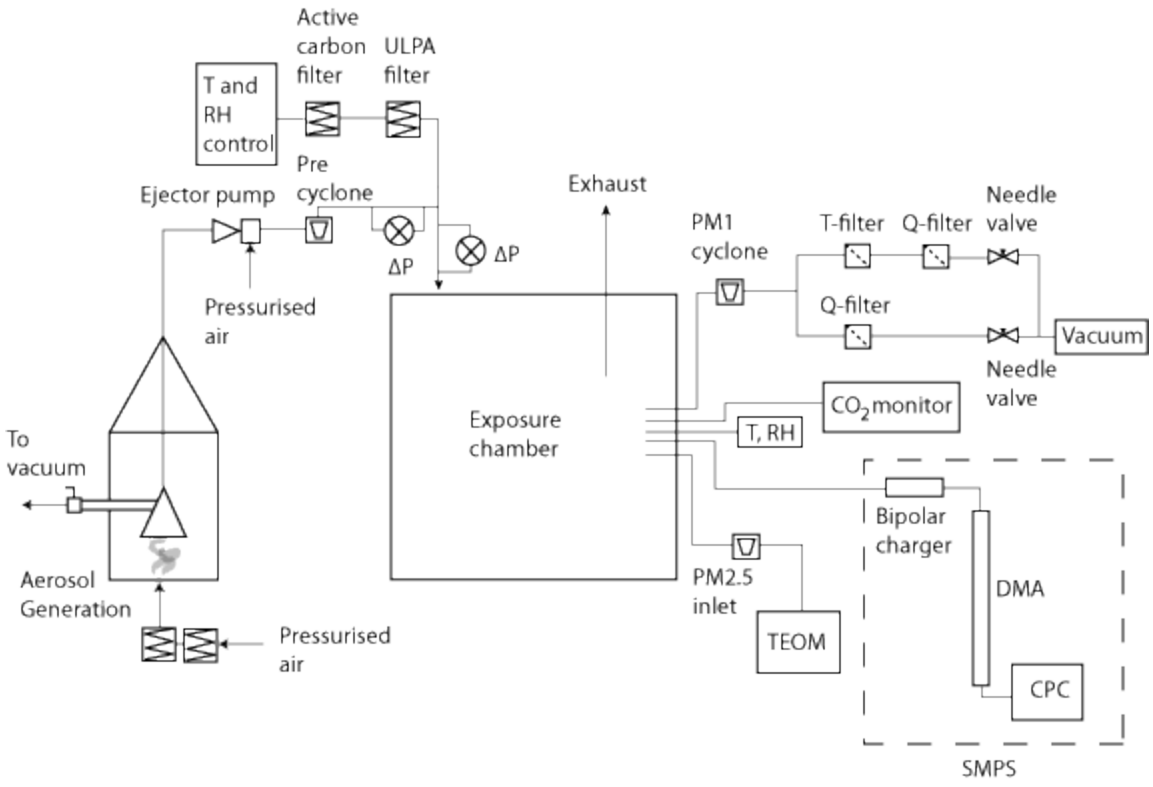

Figure 4.4. Schematic view of the complete human exposure system, including aerosol generation.

The aim was to create an aerosol generation system which can provide a desired aerosol in terms of concentration, size distribution and chemical composition to the exposure chamber. This demands a generation volume which provides enough space to generate the desired aerosol, enough capacity to transport the aerosol from the generation chamber to the exposure chamber in short time, and possibility to control the concentration of aerosol in the transport system.

The chosen aerosol generation system (figure 4.4) consists of a glass and stainless steel chamber with a total volume of 1.33 m^3, see figure 4.5. The bottom surface is 0.81 m^2 which is an area big enough to generate several different aerosols, including those whose generation method is space demanding, and with room enough for additional devices that are needed for achieving the desired results, such as a fan to control the air movements in

the generation volume. There is an inlet for filtered, pressurized air in the bottom of the chamber to provide a steady controlled flow through the generation volume. Before entering the generation chamber this air is directed through a HEPA filter and an active carbon filter, both filters constructed to function under elevated pressure.

The generated aerosol is captured by an extractor hood with an inlet area of 0.39 m x 0.16 m. This hood is connected to a copper pipe, 3 cm in diameter, with the length of 8.25 m, through which the aerosol with the help of an ejector pump[6] (*Coval, model M10*) is transported into the exposure chamber. The pump draws 400 lpm of aerosol from the generation volume and delivers 500 lpm after dilution (at 5 Bar) with filtered pressurized air. These flow-rates can be varied by adjusting the operating pressure of the vacuum ejector. The extractor hood and ejector pump is used for keeping the residence time of the aerosol in the generation system at a minimum. Preliminary experiments showed that letting the aerosol travel the distance to the outlet in the top of the generation chamber by convection alone provided too long time for it to age, resulting in a non-relevant size distribution and strongly reduced number concentrations. The main aerosol process one wants to avoid here is coagulation, which easily occurs with high number concentrations and long residence time. Coagulation changes the number size distribution towards larger and fewer particles, neither of which is desired in these exposure experiments. In principle we wanted to achieve a dilution process (residence time and dilution ratio) relevant for that occurring in realistic indoors and industrial environments.

The concentration of aerosol transported out of the generation chamber can be varied by opening a valve in the extractor hood (figure 4.4), which lets a desired amount of the aerosol pass to the outgoing ventilation system instead of into the exposure chamber. Downstream the ejector pump is a cyclone, the purpose of whichis to separate any particles bigger than a couple of micrometers. This is important since particles which have deposited in pipe bends and in the ejector may become resuspended by the air flow. Such mechanically generated particles would mainly be in a size range larger than 2-3 μm, and should be prevented from entering the exposure chamber, as the exposures of welding fume and candle smoke occur mainly as fine particles.

The aerosol flow into the filtered air flow provided from the temperature and relative humidity control unit (typically 1800 lpm) can be determined from pressure drop measurements by an iris, and so, by the same mean, can the total flow into the exposure chamber (typically 2100-2300 lpm). Upstream the ejector pump a DustTrak can be connected to provide an estimate of the generated aerosol mass concentration. This turned out to be very valuable in assuring that the welding smoke output was similar at different exposures.

[6] The ejector pump is a construction that uses the venturi effect to convert the pressure energy of a first air flow to kinetic energy. This creates a low pressure zone that draws in a second air flow (the aerosol) and then recompresses the air mixture; hence both transport and dilute the generated aerosol.

Figure 4.5. Aerosol generation system. The hole on the front is used to start a generation and is then covered with a plastic sheet to ensure no contamination of the aerosol or of the laboratory air.

The air surrounding the generation chamber is protected from contamination by a hatch in the front of the chamber which only is open during the short time the generation is initiated. This combined with the throughput of the extractor hood keeps any traces of the generated aerosol from entering the space around the chamber, thus providing the possibility for double blind human exposures. Moreover, the generation chamber is placed behind screens in a room separated from the room of the exposure chamber.

4.1.2.1 Generation of candle smoke for human exposure

Blue tapered candles of a common type were purchased in a local retail shop. These candles consist of a mixture of stearin and paraffin (these are the same candles extensively characterized by Pagels et al. 2008). With the help of a rotating fan (Appliance, Model AFT-25) set at 140 V in the generation chamber the candles are made to flicker and hence produce some elemental carbon (soot).

A simple box model (Pagels et al., 2008) was applied for estimating the mass emission factor from the measured particle concentrations in the chamber. Assuming that the air in the chamber is well mixed the following mass conservation relationship can be applied:

$$\frac{dC(t)}{dt} = aC_{inc} + \frac{E_{r,m}}{V_R} - (a+\beta)C(t) \qquad (4.6)$$

Where $C(t)$ is the concentration in the chamber, $C_{inc.}$ is the concentration in the incoming air, a is the air exchange rate (h^{-1}), β is the sum of other loss mechanisms (h^{-1}), for example wall losses, $E_{r,m}$ is the mass emission factor (mg/h) and V_R is the volume of the chamber. Assuming that C_{inc} and that the initial concentration can be set to zero, eqn. (4.6) has the following solution:

$$C(t) = \frac{E_{r,m}}{V(a+\beta)} \cdot \left(1 - e^{-(a+\beta)\cdot t}\right) \tag{4.7}$$

4.1.2.2 Generation of welding fume aerosol for human exposures

The welding fume was generated using a Kempomig 350 welding system with a 1 mm ESAB Aristorod 12.50 electrode fed through the nozzle at 3 cm/s (see Appendix G for technical specifications). This electrode is widely used in the welding industry, for example at one of the investigated welding workshops. The substrate was mild steel, which is the type of steel most commonly used in the industry (http://steel.keytometals.com). An *Air Liquide Arcal* MAG Ar/CO_2 shielding gas mixture, at a flow of 12 lpm, was used. This is the mixture recommended for MAG welding in mild steel. Welding is done at 125 A, 5.5 V. These settings, in combination with the electrode feed rate, render a smooth, even and reproducible welding joint. The welding nozzle is moved at a steady speed over the substrate and care is taken not to let a new welding joint cross an old one. A trained welder was present during the initial phase of the welding work, when the method was established and the welding equipment settings were chosen. Welding is not performed constantly during an exposure event but rather periodically. A welding pulse of three minutes is generated followed by a non-welding period of 15 min. This is due to practical reasons but it can be noted that non uniform exposures resemble real life work situations, like figure 3.10 shows. Constant monitoring with the TEOM and SMPS system during the exposure day allows the length and frequency of these periods to be adjusted to fit the desired mean concentration.

4.1.2.3 The exposure events

The exposure studies are conducted in groups of three persons at a time. Each group attends the event at two occasions, one when they are being exposed to the aerosol and one when they are being exposed to particle free filtered air. In the initial part of the project there were four occasions with exposure and four blank occasions for both candle smoke and welding fume. The candle exposure events are 3 hours long, preceded and followed by health checkups of the human test subjects (see Appendix F for detailed exposure schedules). The welding fume exposures are 5 hours and 20 minutes long, interrupted by a 1.5 hour lunch break, during which the human test subjects did not only have lunch but also got their respiratory tract deposition of particles determined by the RESPI system (described in Appendix C). The group is not being informed of which exposure that occurs, neither are the medical staff; the only persons who have this information are the persons working with the generation. To as far as possible avoid any means for others to determine if it is a blank occasion or not, the aerosol is generated in both cases but not led into the exposure chamber on blank days. To not, from inside the exposure chamber, making it possible to judge whether the ejector pump is on or not, a silencer is placed on the aerosol transport system just before its inlet to the chamber.
The armchairs and tabeles used in the exposure chamber were baked off in 50 ^{o}C for several hours, to ensure that volatile organic compounds will be emitted from them during the exposures.

4.1.3 Measurement instruments

4.1.3.1 SMPS

An SMPS (Scanning Mobility Particle Sizer) system measures the size distribution of sub micrometer aerosols using an electrical mobility separation technique, with optical particle detection. The main components of the systems are the DMA (Differential Mobility Analyzer) and the CPC (Condensation Particle Counter), see figure 4.7.

The purpose of the DMA is to remove a known size fraction of an incoming polydisperse aerosol by the use of a variable high-voltage power supply. It consists of a bipolar charger and an electrostatic classifier. The bipolar charger – also called neutralizer – exposes the aerosol particles to high concentrations of bipolar ions, thus giving the particles a bipolar equilibrium charge distribution. The charged aerosol passes from the neutralizer into the electrostatic classifier, which consists of two concentric metal cylinders. The flow of polydisperse aerosol and another flow of filtered sheath air are introduced at the bottom of the DMA used in our experimental setup and travel up the annular space between the cylinders (the sheath air closer to the inner cylinder – called the collector rod - and the aerosol closer to the outer cylinder). The flows are laminar, hence the particles in the aerosol flow do not mix with the clean sheath flow. The collector rod is maintained at a controlled, but variable, negative voltage, and the outer cylinder is electrically grounded. The electric field which is thus created between the two cylinders causes positively charged ions to be attracted to the negatively charged

collector rod. Where on the length of this rod the particle end up depends on the particle electrical mobility, the flow rate and the geometry of the construction.

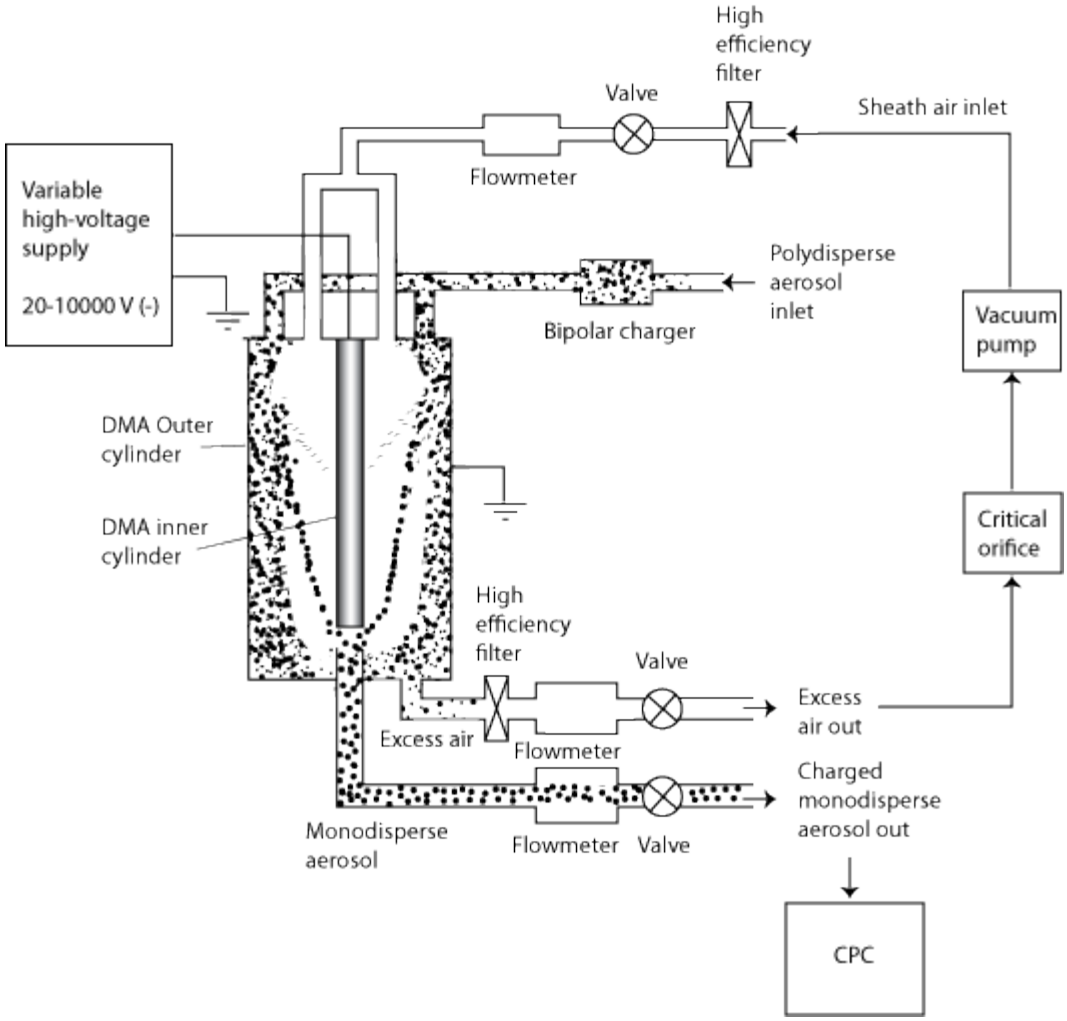

Figure 4.7. The Scanning Mobility Particle Sizer system (After *TSI* product information).

Particles with a high electrical mobility are precipitated lower down along the rod than those with lower electrical mobility. Particles within a narrow range of electrical mobilities exit through a small slit at the top of the collector rod. When the voltage is varied, particles with different electrical mobility exit exactly at the slot, thus applying a voltage ramp from, for example, 20 to 10 000 volts, will render a size distribution covering the major part of most aerosols from combustion or other chemical processes.

A particle with a certain mobility may exist as a small particle with a single charge or as a larger particle with multiple charges, either having the same electrical mobility thus being removed at the slot at the base of the collector rod by the same voltage. This is compensated for by the system's software. Once the particles are classified according to electrical mobility, their concentration is measured by a CPC, which detects single particles on a continuous basis (figure 4.8). When entering the CPC, the sample passes

through a saturator block, where alcohol (n-butyl) evaporates into the sample stream, making the flow saturated with alcohol vapor. Then the sample passes into a condenser tube where it's cooled by a thermoelectric heat pump, causing the alcohol vapor to supersaturate and condensate onto the particles (regardless of their chemical composition). As the droplets exit the condensor they pass through a diode laser (780 nm), and the light scattered by these droplets is collected by optics and focused onto a photo detector. The detector converts the light signal to an electrical pulse, which is recorded as a particle count.

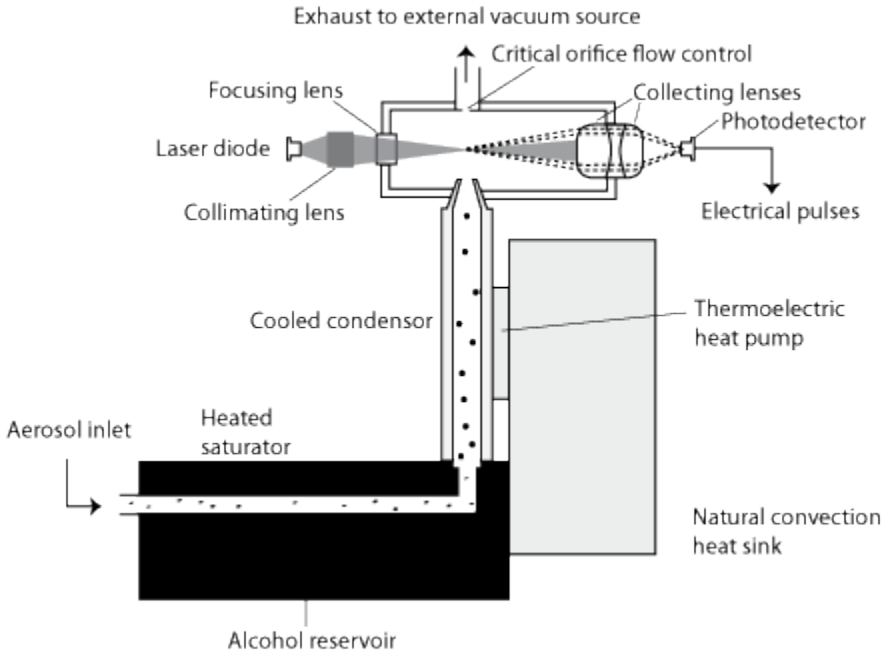

Figure 4.8. Schematic view of a Condensation Particle Counter, CPC. (After *TSI* product information).

The SMPS system employed to extract and analyze sample air from the exposure chamber during the experiments and the exposure events, consist of a CPC (*model 3010, TSI Inc.*) and a long column DMA (*Hauke DMA*) with a length of 28.00 cm. The flow of aerosol through the CPC is 0.50 lpm, (achieved by adding a 0.5 lpm supply flow of filtered air to provide the full 1.0 lpm demanded by the CPC) and the sheath flow through the DMA is 5.0 lpm. Critical orifices are used downstream both the DMA and CPC to assure stable flows. A scantime of 120 s is used. These settings renders 38 size intervals with geometric mean diameter between 10.3 nm and 718,2 nm. The data is processed by a Labview software (written by Dr. Jingchuan Zhou and MSc. Jakob Lönndahl, Lund University) which provides number concentration (#/cm^3), surface concentration ($\mu m^2/cm^3$), volume concentration ($\mu m^3/cm^3$) and size distribution.

4.1.3.2 TEOM

The TEOM (Tapered Element Oscillating Microbalance, Rupprecht & Patashnick Co. Inc.) is a continuous, filter-based method for aerosol mass measurements. The tapered element is hollow, made of glass and oscillates at its eigenfrequency (figure 4.9). A filter is placed on top of the element. When the sample flow passes the filter, particulate matter is deposited, causing the weight of the filter to increase and hence the oscillation frequency to decrease proportionally to the increase of filter mass, according to:

$$\Delta M(g) = K_0 \left(\frac{1}{f_1^2} - \frac{1}{f_0^2}\right) \quad (4.8)$$

The sample flow passes through the hollow element to an active volumetric flow control and a vacuum pump, to maintain constant flow, making it possible to translate frequencies to particle mass concentrations.

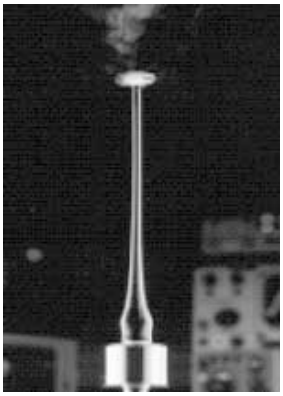

Figure 4.9. The oscillating tapered element in the TEOM.

The sample air is pre heated to 50.00 ^{o}C (by default) to avoid mass fluctuations due to variable water contents in the aerosol. The sampled particle fraction is decided by the PM inlet used, possibilities are PM10, PM2,5 or total suspended particulate matter (TSP). In our project a PM2.5 cyclone was being used.
The TEOM has a high time resolution – down to less than 30 s – and the data is primarily stored as half hour or one hour average mass concentration values. The detection limit is less than 1 µg/m^3. The instrument is quite sensitive to vibrations, and needs a time for stabilization of about an hour or two after having been moved.

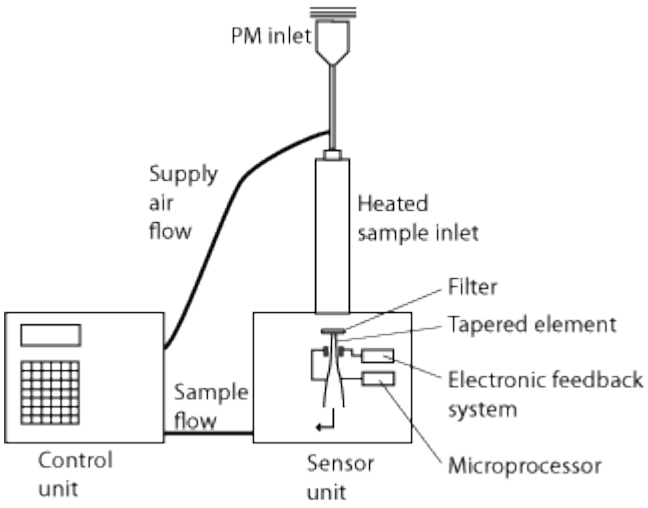

Figure 4.10. Schematic view of the TEOM system.

The TEOM used in the exposure chamber setting has a time averaging set to 1 min, to provide a quick response of the concentration fluctuations that occur, especially during the welding sessions. Data from the TEOM is being processed in a custom-written Labview program that feeds us with the mean mass concentration, from the start of the exposure event in question. From this value we estimate how long the next welding pulse should be.

4.1.3.3 DustTrak

A DustTrak measures aerosol mass concentrations for particles in the range 0.1 to 10 µm in real time with the help of a photometer that detects scattered laser light off the particles. The instrument can detect mass concentrations down to 0.001 mg/m^3. The DustTrak has been used in close connection to the fume extraction hood to provide a primary monitoring in real time of which aerosol mass concentration is being supplied into the chamber. It should be noted that the DustTrak gives a very rough estimate of the true mass concentration, but for a given aerosol it can be used with high precision for relative measurements. Its advantages are its fast time-response and the fact that it can be used over a very large concentration range (0.001 to 100 mg/m^3).

4.1.4 Chemical characterization of exposure aerosols

The aerosol chemical composition of the two particle sources was characterized mainly by two methods: PIXE (Particle Induced X-ray Emission) and OC/EC (Organic Carbon/Elemental Carbon) analysis.

PIXE is a method in which a focused proton beam of 2.55 MeV (Pallon J, 2008) creates a vacancy in an inner electron shell of an atom, which put the atom in a state of high excitation. A transition to a state of lower energy quickly occurs when an electron from an outer shell falls into the vacancy to fill the hole. The electron hole can thus be seen as moving outwards to outer shells and a series of emission lines, corresponding to the successive atomic energy losses, is obtained. The cross section for the creation of an

inner shell vacancy is very high using protons and therefore the sensitivity is high – most elements except the very light ones (Z < 14) can be detected in concentrations below 1 ppb (Svanberg S, 2003).

For organic and inorganic carbon content of the chamber air particles filter samples are collected (figure 4.11). The air is first led through a cyclone that removes particulate matter larger than 1 µm, (95 % of soot and welding fume particles are smaller than this) then led through two parallel lines whose flow rate are controlled by needle valves. In one of the lines a quartz filter is placed which collects carbon in both particle- and some gas phases. Since the purpose is to gain knowledge of the carbon contents of the particles only the second line has a Teflon filter upstream of a quartz filter. The Teflon filter collects all particulate matter leaving only carbon in gas phase to be collected on the quartz filter. By subtracting the back-up quartz filter from the first quartz filter the total particulate carbon is obtained. In the analysis following the collection procedure, the elemental carbon in the particles are separated from the organic carbon. The analyzer used is Model 2001 Thermal/Optical Carbon Analyzer from *Desert Research Institute.*

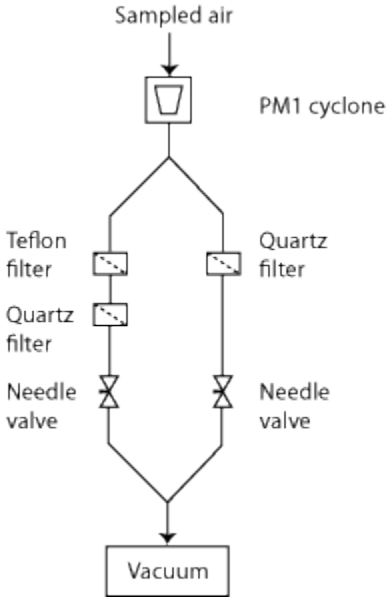

Figure 4.11. Schematic view of the sampling system for OC/EC analysis.

5. Results and Discussion

5.1 The Exposure Chamber

5.1.1 Air Exchange Rate and mixing

5.1.1.1 Calculations of AER and mixing using trace gas

Trace gas is used to calculate the AER in the chamber using both internal fans (fan setting "2") of the ventilation system and an iris setting of 3, respectively to calculate the AER when the express fan is used.

Using the normal ventilation system at its highest air flow setting, the AER calculations from the three channels of the trace gas monitor resulted in an average of **4.3 h^{-1}**.

Two situations are evaluated using the express fan, these are (1) directing the exhaust air via the ante chamber on its way out and (2) directing it directly out from the exposure chamber.
Curve fitting to a straight line in Matlab results in an average value of the air exchange rate for the three measure points of **14.4 h^{-1}**. The air exchange value when the exhaust air flow was redirected to not pass via the ante chamber was **13.1 h^{-1}**.

For chamber characterization it is also of interest to know whether the mobile fan inside the chamber needs to revolve to meet the criterion of complete mixing of the chamber air. For examining this, another set of trace gas experiments were being conducted.
First the mobile fan was set to 80 V, then after 10 min the setting was reduced to 70 V, which is the lowest possible voltage value for the fan to still revolve. Both fans in the ventilation systems were on (fan setting "2") and the iris was set to 3, indicating an air exchange rate of about 4 h^{-1} according to previous calculations. In figure 5.1 the differences in measured concentration is illustrated. The concentration values recorded in channel 1 is here considered to be the value which the total volume of air in the chamber should acquire if the mixing had been instantaneous, and the deviation in percent from this is calculated for the other two channels.
It seems that the two different fan settings do not affect the air mixing considerably; the deviation from the inlet aerosol is around 10 % for the both different voltage settings.

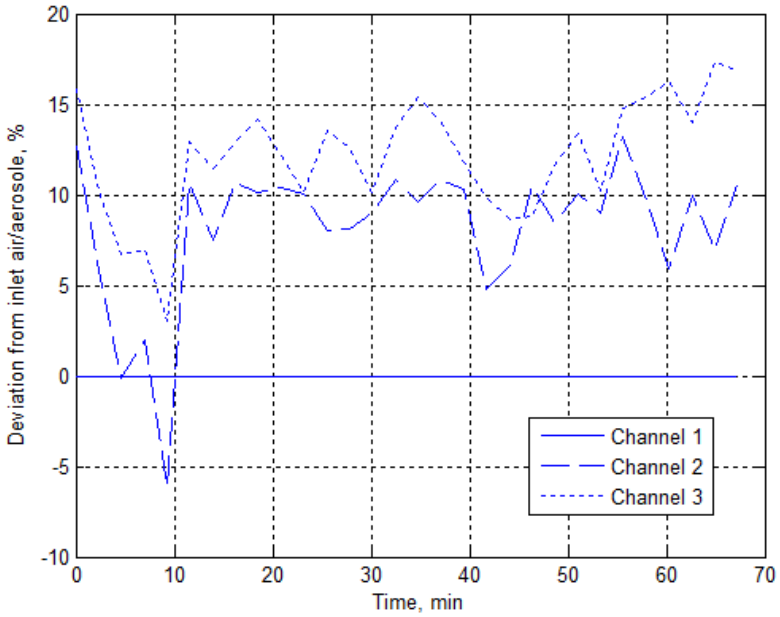

Figure 5.1. Concentration differences between the three measurement points.

Consecutively the mixing without revolving fan, when the mixing in the chamber is due solely to the ventilation system itself, is evaluated at an air exchange rate of 4 h^{-1}.
The result can be seen in figure 5.2. The deviance from the initial concentration is about 5 % in one measurement point and 10-15 % in the other.

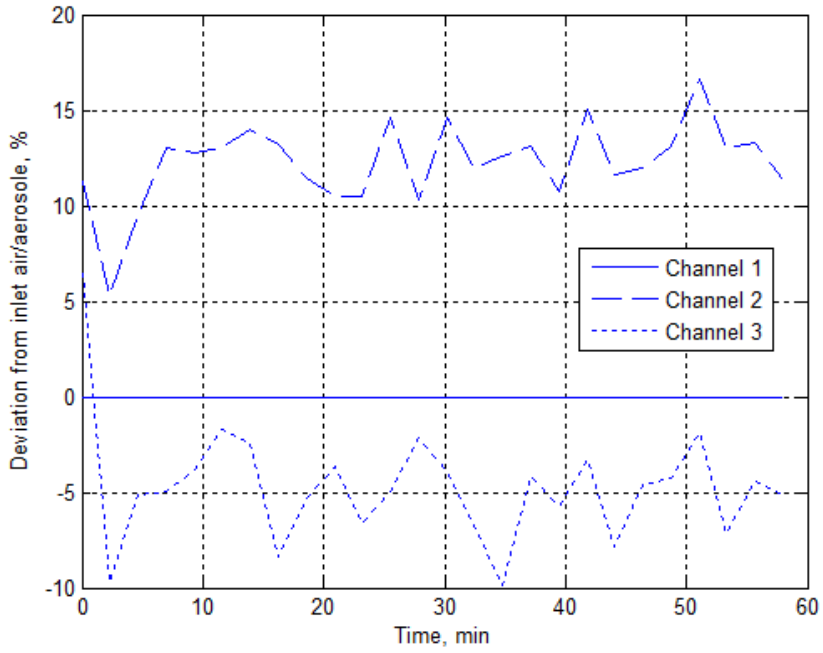

Figure 5.2. Concentration differences between the three channels.

Comparing to the experiment with the rotating fan, where the ventilation and iris settings are the same as in this experiment, it is apparent that the mobile fan does not contribute significantly to the mixing of the air volume.

The outcome of this experiment is that the chamber can be used without the internal fan at air exchange rates around 4 h^{-1} with concentration gradients below 15 %.

5.1.1.2 Calculations of AER using pressure drop over an iris

To achieve an air exchange rate of approximately 4.5 h^{-1} an air flow of about 100 m^3/h is needed. By consulting a diagram (provided by the iris manufacturer) it is apparent that an adequate pressure drop is obtained by setting the iris to position 6.5. This renders an experimentally determined pressure loss of 122 Pa over the iris, which gives an air flow of 23.2 l/s using equation (4.5) in the Methods section. This corresponds to an air exchange rate of **3.89 h^{-1}**, which correlates well with the previously calculated value.

The iris is used to examine which air exchange rates are rendered by other flow settings.
Using fan setting "2" of the ventilation system and changing the iris to position 3 an air exchange rate of **4.5 h^{-1}** is achieved (ΔP = 20 Pa).
Maintaining the iris in position 3 and using fan setting "1" render an air exchange rate of **3.07 h^{-1}** (ΔP = 77 Pa).

To attain even lower air exchange rates the air flow is redirected through a rotameter which can be used for quenching the flow (gauge A in figure 4.3). The rotameter, whose accuracy is considered to be only approximate (possibly due to leaks downstream), is varied until a head loss of 19 Pa is achieved, meaning that the air exchange rate is **1.5 h^{-1}** with these settings.

To get an even lower air exchange rate, of about **0.5 h^{-1}**, the air is directed through rotameter B (figure 4.3) instead. It is obvious that to achieve AER of 0.5, which means a flow of 3 l/s, the iris and the flow through the gauge has to be regulated so that a head loss of 11 Pa is obtained. This is gained by an iris position of 8.
Achieving even lower air exchange rates using the present iris is difficult since that does not render a head loss through the iris big enough to be measurable.

5.1.1.3 Calculation of AER using particle concentration data

With the ventilation system set at fan setting "2", particles of NaCl were introduced to the chamber. When a number concentration of approximately 100 000 cm^{-3} was achieved the generation was turned off, and the concentration decay was monitored until the levels were 2000 – 5000 cm^{-3}.

Particles in the size range of 200 nm, which have the lowest probability to diffuse or sediment to the walls with high air flow settings, are monitored and using MatLab, a straight line is fitted to the natural logarithm of $C(t)/C_0$ for the particle sizes around 200 nm, namely 186 nm, 210 nm and 239 nm, see figure 5.3.

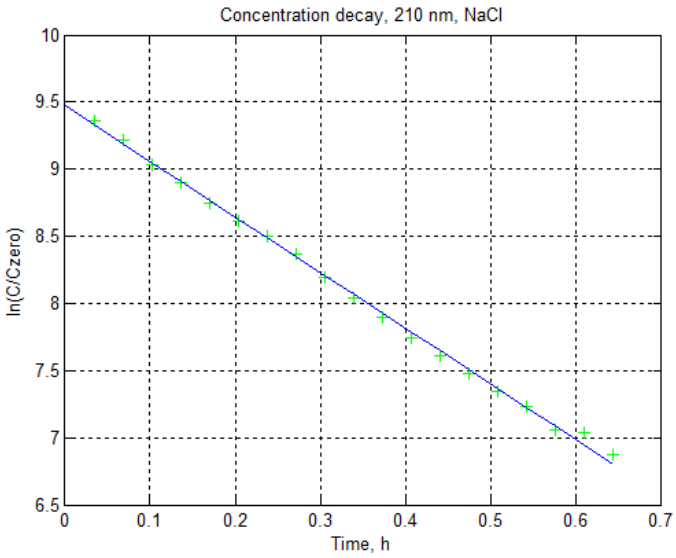

Figure 5.3. Collected data plotted against time for 210 nm NaCl particles together with the curve fitting to a straight line.
Coefficients of slope are calculated for these three size bins are:

186 nm: -4.0607
210 nm: -4.1151
239 nm: -4.2712

This results in an average air exchange rate of **4.15 h^{-1}**.

The results described above are summarized in table 5.1.

Table 5.1. AER rendered by different flow settings with different measurement methods.

Iris-position	Ventilation system	Redirection of the flow	ΔP [Pa]	AER (iris) [h^{-1}]	AER (particle measure-ments) [h^{-1}]	AER (trace gas) [h^{-1}]
3	Fan setting ”2”	None	20	4.5	4.15	4.3
6.5	Fan setting ”2”	None	122	3.9		
6.5	Fan setting ”1”	None	77	3.1		
6.5	Fan setting ”2”	Through rotameter A (43 m^3/h)	19	1.5		
8	Fan setting ”2”	Through rotameter B (13 units)	11	0.5		

5.1.2 Wall deposition

To calculate the wall deposition the air exchange rate is kept at a minimum, using the settings described in section 4.1.1.3. The three channels of the trace gas monitor generated an AER mean value of **0.27 h^{-1}** with these settings.
NaCl particles at a concentration of about 14 000 cm^{-3} was released into the chamber, the concentration decay monitored with an SMPS system and a deposition curve due to diffusion (figure 5.4) was calculated for the different NaCl particle sizes.

It is apparent that smaller particles have a much higher deposition rate than bigger, which is expected (due to the diffusion dependency on particle size). The more turbulent the flow would be in the chamber, the bigger the deposition velocity will be for all sizes.
This curve can be compared to previous works, e g Hussein at al. (2006), where measured deposition values have been compared with values calculated using a model developed by Lai and Nazaroff (2000). The deposition curves obtained by the model is somewhat less steep than the one in figure 4.15, but a room area-to-volume ratio of 3.0 m^{-1} has been used here, while our exposure chamber has an A/V ratio of 2.17, so the graphs are not ideal for comparison.

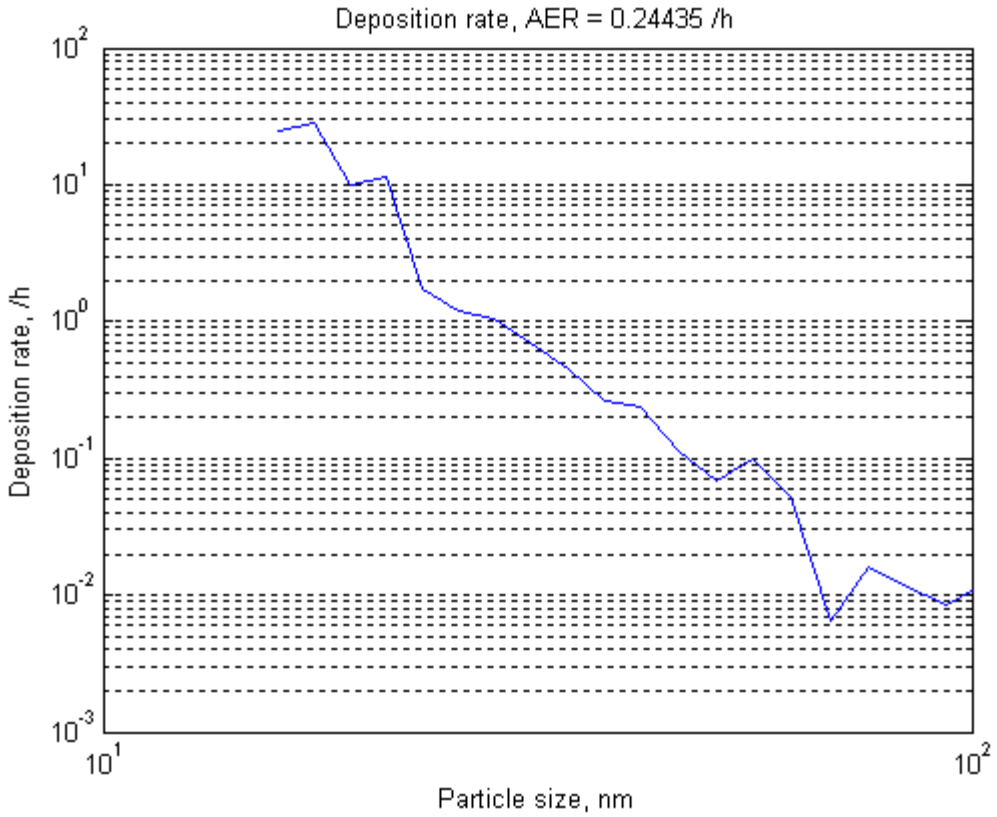

Figure 5.4. Deposition rate for the particle size range studied.

5.2 Aerosol generation

5.2.1 Generation system

The pipes transporting the aerosol and the junctions connecting them are made of copper, assuring durability and a minimum of leakage and electrostatic deposition. The residence time in the system, from extractor hood to exposure chamber inlet, is approximately one second. Keeping this time short is of great value since the quicker the aerosol reaches the dilution point; the more the aerosol dynamic processes (mainly coagulation) are reduced. From the results from both candle smoke and welding fume generation, reviewed below, it is apparent that the generation system is well suited for producing these two high temperature aerosols and delivering them to the exposure chambers in a well controlled way.

5.2.2 The generated candle smoke

Source characterization studies in the same chamber, with the same sort of candles[7] used in the exposure events, resulted a number concentration of $0.27 \cdot 10^6$ #/cm^3 for four candles burning with sooting combustion, and $0.51 \cdot 10^6$ #/cm^3 during steady burn. The mean candle particle concentration during the exposure events were about $0.94 \cdot 10^6$ #/cm^3 (table 5.1).

The use of a mobile, rotating fan in the exposure chamber resulted in that both ultrafine mode particles in the size range of 15-20 nm and soot particles in the size range of 150-250 nm are generated in the same aerosol. During sooting burn and steady burn, mass emission factors are 25 and 1 µg/h respectively. The fan setting used in our setup resulted in a mass emission factor of about 4 µg/h determined from the concentrations in the exposure chamber, i. e. an intermediate burning mode, which we believe is representative for typical indoor exposures. 6-10 candles were used placed under the extraction hood. This ammount of candles gave a mean mass concentration in the exposure chamber of approximately 200 µg/m^3.

Using the box model described in section… for the chamber exposure, with a mean mass concentration in the chamber based on the time period where steady state has been reached (200 µg/m^3) allows us to set the term in parenthesis in eqn. (4.7) to equal 1. The AER in the chamber during the exposure events is 4.5 h^{-1} and the wall deposition can, with this air exchange rate, be assumed to be zero. This leaves us with all factors known, except $E_{r,m}$, which easily can be calculated. The result is a mass emission factor of 1.9 mg/h (for 10 candles) – 3.2 mg/h (for 6 candles).

[7] A dark blue tapered candle made up of a wax containing both stearin and paraffin, studied by Pagels et al (2008)

This shows that we have somewhat of an intermediate mode of burning during the candle smoke generation, which also can be verified by figure…. In this figure we can see that the distribution from the exposure event is similar to a combination of candle II with shield (steady burn) and the same candle without shield (sooting burn). This is likely a result from that the fan is rotating from side to side, sweeping over the set of candles creating a temporary turbulence but leaving the candles in a steady burn the rest of the time. Logically this resembles a real house setting, where candles burning on a table will flicker when persons move about or when a door is opened, but will burn steadily otherwise.

The size distribution for candle smoke particles in the chamber correlated well to that found in recent studies (figure 5.5) (Pagels et al. 2008).

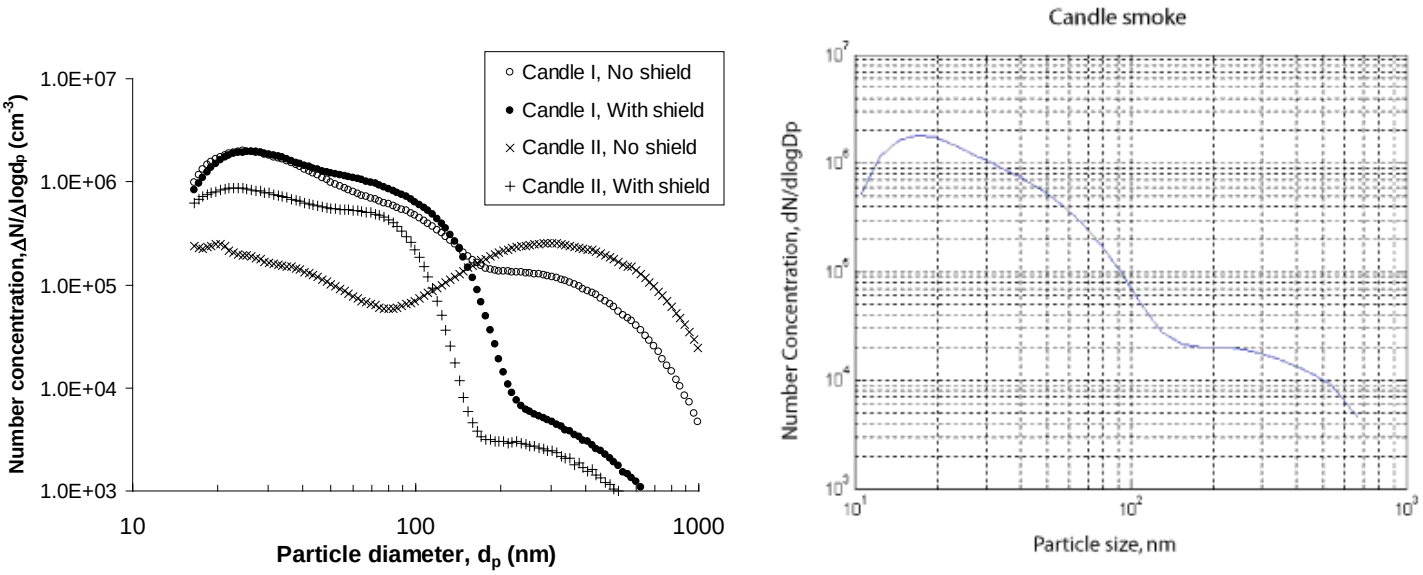

Figure 5.5. Size distributions for candle smoke. The left figure (Pagels et al., 2008) shows how size distribution is dependent on burning mode and candle composition. The right figure shows a mean size distribution during an exposure event.

The result of the box model calculations is compared to Pagels' study, to confirm that the mean mass concentration during the exposure event is at a relevant level, by using known emission factors for steady and sooting burn and see what number of candles that renders a mean mass concentration of 200 µg/m^3 in a home environment.
Typical air exchange rate for an apartment is 0.5 h^{-1}. A room area of 25 m^2 and a headroom of 3 m gives the volume of a normal living room, in which we assume complete mixture of the air. For the wall deposition a mean value from studies made by He et al. (2005) is used: 1.9 h^{-1}. If the emission factors calculated by Pagels et al. (2008) is used this mean mass concentration corresponds to 2 hours steady burn of 12-18 candles or 2 hours sooting combustion of 1-4 candles.

In contrast to the welding fume particle generation, which were made in pulses, the candles burn constantly during the exposure event. This does not ensure a completely constant chamber concentration (figure 5.6) which is due to the fact that candle combustion is a complex process, governed by many factors. In the case of candle burning the emission can be influenced by factors such as the length of the wick and of the candle itself.

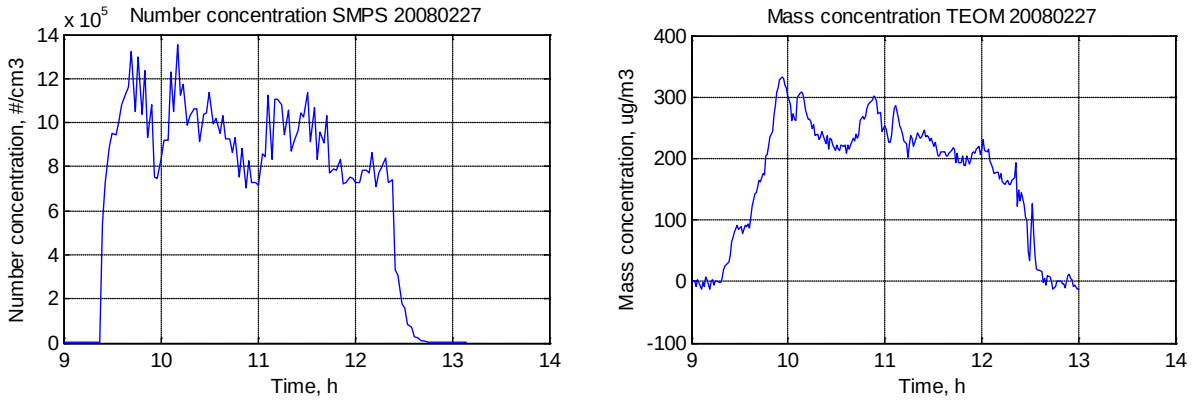

Figure 5.6. Number and mass concentrations during a stearine exposure event. The average number and mass concentrations were 905000 cm^{-1} and 218 $\mu g/m^3$ during this exposure trial. The generation begins at 9.30 and at 12.30 the express fan is turned on.

The chemical composition of the candle smoke generated during the exposures (figure 5.7) is dominated by elementary carbon (68 %), i. e. soot, which is due to the air turbulence created by the rotating fan. The organic carbons can emanate from lighting and extinguishing the candles. Nitrate, potassium and sodium are soluble salts.

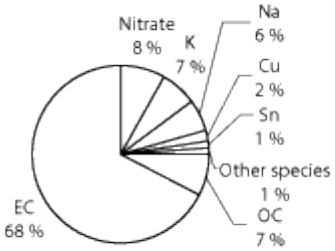

Other species, detected mass (%)
(IC + PIXE)

F	0.63
Cl	1.57
NO	8.42
PO	0.03
SO	0.12
Ca	0.05
Na	5.82
K	7.07
NH	0.46
Cu	1.96
Sn	1.18
Zn	0.03
Fe	0.01
Pb	0.06

Figure 5.7. Chemical composition of generated candle smoke, results from OC/EC, IC and PIXE analysis. IC and PIXE data from Pagels et al. 2008.

5.2.3 The generated welding fume

The concentration during a welding workday varies with time, depending on how intense the activity is. In the workshops the PM10 mass concentration in the background zone could typically vary between 100 µg/m^3 during periods of low activity to 3000 µg/m^3 or above during intense periods (figure 5.8). The workshop personal exposures, measured as respirable dust (less than ~4 µm in aerodynamic diameter), ranged from 600 µg/m^3 to 3400 µg/m^3.

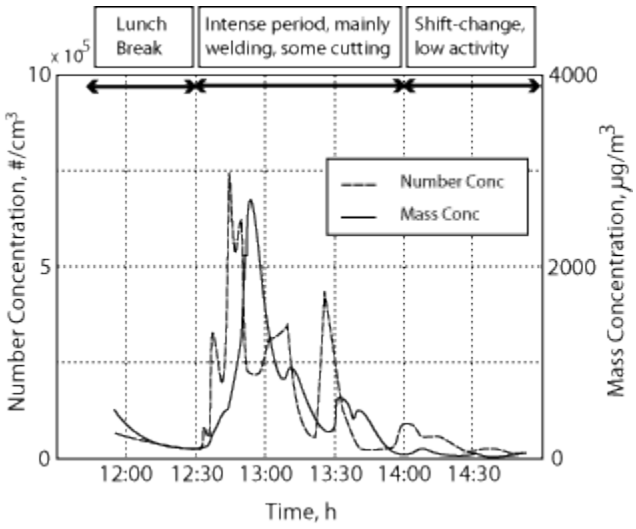

Figure 5.8. Number Concentration fluctuations in the background measurement point during the afternoon at workshop 3. 12:30 lunch break finished, at 14:00 there is a shift change, during this period the activity is low (Isaxon et al., 2008).

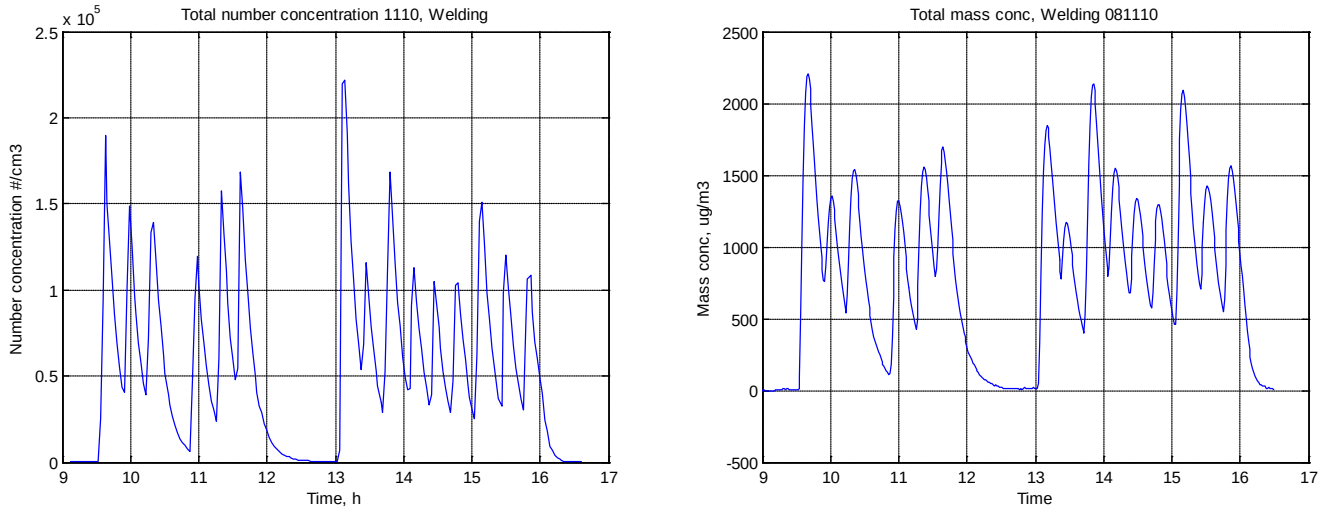

Figure 5.9. Number and mass concentration during one exposure event (20081110). The human test subjects were exposed to a mean mass concentration of 1035 µg/m^3 and a mean number concentration of 74500 cm^{-3}.

Welding in pulses (figure 5.9) during the exposure events rendered a relevant concentration compared to what was measured in the workshops. The mean concentration during the exposure day was kept at approximately 1000 µg/m^3 (table 5.1), well correlated to levels measured at workshops and with a reasonable marginal for not exceeding the manganese health limit value of 100 µg Mn/m^3 during an 8 h period. The manganese level in the chamber was about 85 µg/m^3, according to PIXE analysis.

The size distribution of the generated welding fume is typically a single mode with a peak at 100-200 nm. This corresponds well to what was seen at the in-plume measurements in the welding workshops, as figure 5.10 shows.

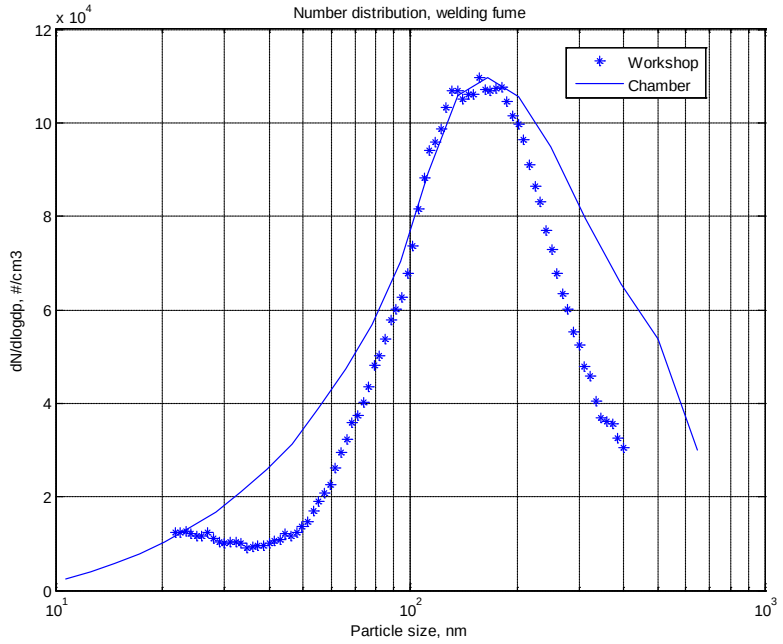

Figure 5.10. Number distributions from laboratory and workshops. Workshop data have been normalized to fit the maximum value of the chamber concentration.

Chemically the welding smoke generated during the exposure events is dominated by metal oxides, foremost iron oxide, expected to be present in the form of Fe_2O_3 (figure 5.11). Another large fraction is manganese, expected to be present as MnO_2. This corresponds well to the composition of workshop welding in mild steel, described in section 3.2.5.

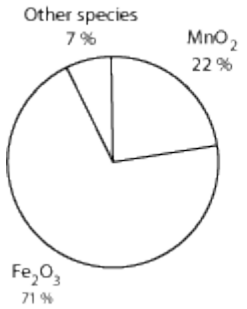

Other species, detected mass (%) (PIXE)	
Si	3.16
S	0.23
Cl	0.67
K	0.12
Ca	0.13
Co	0.10
Cu	1.00
Zn	1.02
Pb	0.65

Figure 5.11. Chemical composition of generated welding fume, results from PIXE analysis.

In table 5.1 the exposure levels for the two aerosols is summarized, together with levels during the blank exposure events.

Table 5.1. Summary of particle number and mass concentration (PM2.5) means during candle smoke and welding fume exposures, with standard deviation.

Exposure type	Number concentration (cm^{-1})	Std dev	Mass concentration (cm^{-1})	Std dev
Candle smoke	907000	± 2120	205	± 24
Candle blank	19.7	±11.4	1.6	± 3.8
Welding fume	67400	± 16000	1000	± 94
Welding blank	17.4	± 9.3	3.1	± 0.5

It is apparent that candle particles are much higher in number concentration than welding fume particles, due to the primary particles generated from this type of combustion (see also figure 5.5). The welding fume particles are rich in metal content (figure 5.11) which is one of the reasons for the higher mass concentration for these particles compared to the ones from the candles. The welding fume particles thus have a higher mass concentration in the gas phase when the particles are formed. Also the welding fume is not diluted at the same rate as the candle smoke, giving the newly formed particles more time to form agglomerates, hence decreasing in number concentration. During the blank exposures the filtered air has provided an almost particle free environment in the chamber, the values in table 5.1 can be compared to normal background levels in a room; 1000 #/cm^3 and 10 µg/m^3 respectively.

6. Conclusions and further work

The aerosol generation method and exposure chamber were found to be a very useful system for 3-6 hour exposures of 3 human test subjects at a time. The aim to have a particle concentration, size distribution and composition during the exposure events that compares with those in real life situations, and with calculations, have been well obtained. We have shown that the procedure is repeatable; using the same method and the same settings renders the same exposure.
The flexibility of the system and the fact that so many parameters can be monitored suggests that it can very well be used for generating aerosols other than candle smoke and welding fume.

The three methods used above provide different approaches to calculating the air exchange rate. The trace gas method is the most reliable one and is therefore considered the reference method. Using both fans in the ventilation system this method gave an air exchange rate of 4.3 h^{-1}. Using salt particles and the same ventilation system settings the air exchange rate was calculated to 4.15 h^{-1}. A thing that can be questioned considering this result is that a somewhat high concentration of particles were used (100 000 cm^{-3}), which could have resulted in coagulation. Using an iris set to 3 rendered an air exchange rate of 4.5 and set to 6.6 an air exchange rate of 3.9. Table 1 shows how varying the air flow and iris setting results in different air exchange rates. This experiment could be developed to obtain a table that suggests how the flow should be directed and the iris set to achieve any desired air exchange rate within the limits of the ventilation system.
Trace gas experiments also showed that there is no need for an internal fan during the exposure events. When adding three humans in the chamber, the internal mixing will be enhanced due to thermal convection added by the energy release from these test persons. In initial exposure experiments the human test subjects experienced a draught even when the rotating fan was at the lowest possible settings, a fact that also contributed to the decision of not using it during the exposures. The decision of what air exchange rate to use during the exposure events is governed by the CO_2-levels. Keeping the concentration of CO_2 lower than approximately 1000 ppm is important for the test subjects comfort and well-being, and this was achieved using an air exchange rate of 4.5 h^{-1}.

A mobile fan does not significantly affect how long time it takes to achieve total mixture in all points in the chamber. The mixing time in the chamber, with or without internal fan, is 10 – 20 minutes which of course is what is expected with AER being 4 h^{-1}. It is of interest to examine this with furniture present in the chamber to ensure that there is no stagnation point anywhere.
The wall deposition is biggest for small particles due to diffusion, which has a big significance for small particle sizes as shown in the Stokes-Einstein equation. The deposition velocity variation has not yet been examined for varying air exchange rates in our chamber settings.

During the next phase in the exposure project particles generated from chemical reactions between terpenes ond ozone will be used as exposure source. A short literature study (appendix E) has been made to base the generation design work on.

7. Acknowledgements

It is most pleasant, interesting and inspiering to be a student at Ergonomics and Aerosol technology. I am greatful to each and everyone who have contributed to this athmosphere. Some people deserve special thanks:

My supervisor Joakim Pagels, for always answering all my questions with the patience of an angel, no matter how busy you are. For encouragement, for being a good and caring friend and for everything you have taught me.

Mats Bohgard, for giving me responsibilities and tasks that truly have made me grow. My employment here is thanks to you, I am so very grateful for this.

Anders Gudmundsson, for always seing solutions instead of problems, for having such an open attitude towars everyone and everything, and for inspiration and support.

Andreas Dahl, for helping out with so many things, practical and theoretical. And for good concert company and for many laughters.

Aneta Wierzbicka, for always taking your time to explain problems I have had, for finding facts I have needed and for being such a truly clever and nice person.

Pontus Roldin, Jakob Löndahl and Erik Nilsson for explaining difficulties and answering questions, every time.

Jan-Eric Karlsson for introducing me to the world of welding.

Eva Assarsson and Katrin Dierschke for explaining all those medical terms for me.

Karin Öhrvik for solving all my problems of administartive nature.

Robert Olsson for saving the data on my harddrive when my laptop crashed. I have now learned the advanatges of doing backups!

My children Loke and Clea, for understanding that I have not always had time to be with you as much as I should have wanted. And to their father Joachim and to my parents Barbro and Roland for helping out with them so many times when I have been busy.

Leif Lönnblad, for proof-reading the manuscript and presenting your opinions in the most pedagogical way. And for, among many other things, serving the best morning coffee ever!

The exposure research project is funded by FORMAS, the Swedish Research Council for Environment, Agricultural Sciences and Spatial Planning and by FAS, the Swedish Council for Working Life and Social Research.

References

Akselsson R., Bohgard M., Gudmundsson A., Hansson H-C., Martinsson B., Svenningsson B., *Aerosoler* Lunds Tekniska Högskola & NOSA, 1994

Antonini J.M., *Health Effects of Welding*, Critical Rewiews in Toxicology, 33(1):61-103, 2003

Antonini J. M., Afshari A. A., Stone S., Chen B., Schwegler-Berry D., Fletcher W. G., Goldsmith W. T., Vandestouwe K. H., McKinney W., Castarova V., Frazer D. G., *Design, construction and characterization of a novel robotic welding fume generator and inhalation exposure system for laboratory animals*, Journal of Occupational and Environmental Hygiene 3 (4): 194-203, 2006

Borghi R., Destriau M., *Combustion and Flames, chemical and physical principles*, Éditions Technip, Paris, 1998

Bratz, Tina, utbildad svetsare, samtal oktober 2007

Burtscher, Heinz, *Properties of Combustion particles*, University of Applied Sciences, Northwestern Switzerland, www.akpf.org/pub/2007_hdt/burtscher.pdf. Downloaded 081120

Classification of Carbon and low-alloy steels, http://steel.keytometals.com/Articles/Art62.htm. Downloaded 081106

Ebersviller S. M., Sexton K. G., Naess E. P., Galloway K. E., Jeffries H. E., *A comparison of the Oxidation Products and Secondary Organic Aerosol Formation Potential of d-Limonene and an Off-the-shelf Cleaning Product Containing d-limonene*, Poster

Environment Agency, http://www.environment-agency.gov.uk/business/444255/446867/255244/substances/1044/?&lang=_e , downloaded 070928

FORMAS, the Swedish Research Council for Environment, Agricultural Sciences and Spatial Planning, http://www.formas.se/formas_templates/Page_556.aspx, Downloaded 080311

Goller J. W. and Paik N. W., *A Comparison of Iron Oxide Fume Inside and Outside of Welding Helmets*, American Industrial Hygiene Association Journal 46(2):89-93, 1985

Gustavsson M., *Experimantal determination of the particle emission from a human being*, MSc Thesis, Division of ergonomics and aerosol technology, Lund University, Sweden, 2004

He C., Morawska L., Gilbert D., *Particle deposition rates in residential houses*, Atmospheric Environment, 39:3891-3899, 2005

Hinds W. C., *Aerosol technology – properties, behavior and measurement of airborne particles*, John Wiley & Sons Inc., New York, 1999

Hussein T., Glytsos T., Ondracek J., Dohanyosova P., Zdimal V., Hämeri K., Lazaridis M., Smolik J., Kulmala M., *Particle size characterization and emission rates during indoor activities in a house*, Atmospheric Environment 40:4285-4307, 2006.

Ichitsubo H., Yamada Y., Shimo M., Koizumi A., *Development of a radon-aerosol chamber at NIRS – general design and aerosol performance*, Journal of Aerosol Science Volume 35 2:217-232, 2004

Isaxon C., Pagels J., Gudmundsson A., Asbach C., John A., Kuhlbusch T. A. J., Karlsson J. E., Tinnerberg H., Kamner R., Nielsen J., Bohgard M., *Welding fume generation for controlled human exposure studies in chamber – comparison with detailed work place measurements*, Proc. of European Aerosol Conference 2008 (2008a).

Isaxon C., J., Gudmundsson A., Asbach C., John A., Kuhlbusch T. A. J., Karlsson J. E., Tinnerberg H., Kamner R., Nielsen J., Bohgard M., *Characteristics of Welding Fume Aerosol Investigated in Three Swedish Workshops*, Conference abstract for Inhaled Particles X, 2008 (2008b).

Jenkins N.T., *Chemistry of airborne particles from metallurgical processing*, Massachusetts Institute of Technology, 2003

Jenkins N. T., Mendez P. F., Eagar T. W., *Effects of Arc Welding Electrode Temperature on Vapor and Fume Composition*, Proceedings of Trends in Welding Conference, ASM, Materials Park, OH, 2005

Jenkins N. T., Pierce W. M.-G., Eagar T. W. *Particle Size Distribution of Gas Metal and Flux Cored Arc Welding Fumes*, Welding Journal 2005

Jenkins N. T. & Eagar T. W., *Chemical Analysis of Welding Fume Particles*, Welding Journal 2005

Kalliomaki P. L., Kalliomaki K.,Rahkonen E., Aittoniemi K., *Lung retention of welding fumes and ventilatory lung functions, A follow-up study among shipyard welders*, The Annals of Occupational Hygiene, 27:449-452, 1983

Lai A. C. K. & Nazaroff W. W., *Modelling indoor particle deposition from turbulent flow onto smooth surfaces*, Journal of Aerosol Science Vol 31 No 4 pp 463-476, 2000

Liu X., Mason M., Krebs K., Sparks L., *Full-Scale Chamber Investigation and Simulation of Air Freshener Emissions in the presence of Ozone,* Environ. Sci. Technol. 38:2802-2812, 2004

Löndahl J., Massling A., Pagels J., Swietlicki E., Vaclavic E., Loft S., *Size-resolved Respiratory Deposition of Fine and Ultrafine Hydrophobic and Hydroscopic Aerosol Particles during Rest and Exercise.* Inhalation Toxicology, 19:109-116, 2007

McDonald J.D., White R. K., Barr E. B., Zielinska B., Chow J. C., Grosjean E., *Generation and Characterization of Hardwood Smoke Inhalation Exposure Athmospheres,* Aerosol Science and Technology, 40:573-584, 2006

MIG/MAG Welding guide, Lincon Electric, 1997

Pagels J., Wierzbicka A., Nilsson E., Isaxon C., Dahl A., Gudmundsson A., Swietlicki E., Bohgard M., *Chemical Composition and Mass Emission Factors of different Particle types present in Candle Smoke*, 2008

Pallon Jan, *Description of PIXE results file*, PIXE laboratory, Nuclear physics, Lund University

Palm O. & Sörnmo L., *Elektrokardiologi, klinik och teknik*, Studentlitteratur, 2008, ISBN 91-44-00615-2

Park K., Cao F., Kittelson D. B., McMurry P. H., *Relationship between Particle Mass and Mobility for Diesel Exhaust Particles*, Environmental Science and Technology, 37:577-583, 2003

Quimby B. J. & Ulrich G. D., *Fume Formation Rates in Gas Metal Arc Welding*, Welding Journal 78(4): 142-149, 1999

Redding C. J., *Fume model for Gas Metal Arc Welding*, Welding Journal 95s-103s, 2002

Rohr A. C., Weschler C. J., Koutrakis P., Spengler J.D., *Generation and quantification of Ultrafine Particles through Terpene/Ozone Reaction in a Chamber setting*, Aerosol Science and Technology 37:65-78, 2003

Singer B. C., Coleman B. K., Destaillats H., Hodgson A. T., Lunden M. M., Weschler C. J., Nazaroff W. W., *Indoor Secondary Pollutants from Cleaning Product and Air Freshener use in the presence of Ozone*, Atmospheric Environment Vol 40, 35:6696-6710, 2006

Singer B. C., Destaillats H., Hodgson A. T., Nazaroff W. W., *Cleaning products and air fresheners: emissions and resulting concentrations of glycol ethers and terpenoids*, Indoor Air 16:179-191, 2006

Svanberg Sune, *Atomic and Molecular Spectroscopy, Basic Aspects and Practical Applications, 4th edution*, Springer, 2003, ISBN 3-540-20382-6

Walsh B. K., Vaughan J. Hunt J., *Providing oxygen therapy during exhaled breath condensate collection using the Rtube*, University of Virginia Pediatric Respiratory Medicine; Charlottesville, Virginia.http://www.healthsystem.virginia.edu/internet/respiratory/research/adding-oxygen-to-the-rtube.doc. Downloaded 081122

Weschler C. J., *Ozone in Indoor Environments: Concentration and Chemistry*, Indoor Air 10:269-288, 2000

Wikipedia, welding. http://en.wikipedia.org/wiki/Welding. Downloaded 070925

Wierzbicka A., Gudmundsson A., Pagels J., Dahl A., Löndahl J., Swietlicki E., Bohgard M., *Characteristics of Airborne Particles in Various Swedish Indoor*, To be submitted for publication

Wierzbicka A., *What are the characteristics of airborne particles that we are exposed to? – Focus on Indoor Environments and Emissions from Biomass Fires District Heating*, Doctoral thesis, 2008

Zimmer A. T. & Biswas P., *Characterization of the aerosols resulting from arc welding processes*, Journal of Aerosol Science 32: 993-1008, 2001

Zimmer A. T., Baron P. A., Biswas P., *The influence of operating parameters on number-weighted aerosol size distribution generated from a gas metal arc welding process*, Journal of Aerosol Science 33: 519-531, 2002

Appendix A

Mean Free Path

If the particle is small and the spacing between the gas molecules is enough, the surrounding gas cannot be treated as a continuous fluid, but must instead be seen as molecules randomly colliding with the particles. The *mean free path*, **λ**, is defined as the average distance traveled by a molecule before colliding, and can be determined by the average distance traveled by one molecule in one second divided by the average number of collisions for that molecule during this time (Hinds, 1999):

$$\lambda = \frac{\bar{c}}{n_z}$$

n_z is given by

$$n_z = \sqrt{2} n \pi d_m^2 \bar{c}$$

where d_m is the distance between the centers of two molecules at the moment of collision. Combining these two equations gives

$$\lambda = \frac{1}{\sqrt{2} n \pi d_m^2}$$

The mean free path for air at STP (293 K and 101 kPa) is 0.066 μm. For a given gas the mean free path depends only on the gas density, meaning that it increases with increasing temperature or with decreasing pressure.

Appendix B

Welding Workshops

The first sampling point was at 2 m height, at least 5 m horizontal distance from the nearest known source of fine and ultra fine particles, using a PM10 inlet, with the purpose of sampling the background air. The second sampling point was in a freshly generated welding plume at a distance 5 – 20 cm above the welding point using a sampling probe immediately connected to a two stage ejector dilution system which provided a fume dilution factor of 1:150. This dilution system was introduced to reduce the magnitude of aerosol dynamics processes (particularly coagulation) and to cool and dilute the sample to the range of the measurement systems. The in-plume measurements provided the signature size distribution and composition for the pure welding fume.

The sampled airflow was led though a splitter to the following instruments: Scanning Mobility Particle Sizer (SMPS, for fine and ultra fine particle size distributions, time resolution of minutes), Fast Mobility Particle Sizer (FMPS, time resolution of 1 second), Aerodynamic Particle Sizer (APS, for coarse particle size distribution), Tapered Element Oscillating Microbalance (TEOM, as a primary measurement for the PM10 mass concentration), Nanoparticle Surface Area Monitor (NSAM, for determining the lung deposited surface area concentration) and two low pressure impactors (LPI); one Hering LPI to collect samples for Transmission Electron Microscopy (TEM) and one Dekati LPI to collect samples for Particle Induced X-ray Emission (PIXE). Some of these instruments are described in more detail in section…To estimate personal particle exposure, selected welders carried personal filter samplers incorporating respirable fraction cyclone pre-collectors (Isaxon et al, 2008).

Appendix C

Medical examinations

Heart Rate Variability

The heart rhythm beat-to-beat variation is part of how the autonomous nerve system regulates the cardiovascular system, both when it comes to how often the sinoatrial node tells the hart to beat and how strong these beats should be. The nervous system can be said to consist of two components; one that has a decelerating effect on the sinoatrial node and is called *parasympaticus*, and one that has an accelerating effect, called the *sympaticus*. The balance between these two activities constitutes the heart frequency. The parasympathic system, which is the dominant one when a person is in a state of rest, can make quick fine adjustments of the occurrence of the upcoming heart beat, whilst the sympathic system is more slow in its actions.

The variations in heart frequency (and blood pressure) in healthy individuals are not random, but consist of certain rhythms that reflect how the autonomous nerve system controls the blood circulation. In HRV analysis the variation in the RR-intervals (see figure …) in a series of heart beats are being studied. Per definition the heart beat begins at the start of the P wave, but using this wave would create an unnecessary amount of noise in the signal.

The signal is analyzed by calculation of its effect spectrum, which reveals how the effect is allocated to the different frequency components in the signal. The effect corresponds to the square of the component's amplitude. The effect spectrum is divided into different frequency domains based on the rhythms the HRV signal is expected to reflect:

1) High frequency (HF) variations (0.15 – 0.50 Hz). Are connected with the breathing pattern and represent parasympathic modulation of the heart frequency.
2) Low frequency (LF) variations (0.05 – 0.15 Hz). Are connected with the blood pressure and represent a combination of parasympathic and sympathic modulation.

Two more frequency components exist; very low frequency (VLF) and ultra low frequency (ULF), but these are not used in the exposure studies due to that the time series are too short.

There is quite a large variation in HRV in between individuals, depending on factors such as age, breathing frequency, mean heart frequency and time of day. The heart frequency variability decreases with increasing age.

If a patient/test subject have a HRV much higher than expected it can be due to extra heart beats or some other rhythm disorder, however it is generally "good" to have a high HRV, and it is when the variability is lower than expected various health disorders can be suspected. Examples of such disorders can be coronary decease, heart attack, cardiac insufficiency or diabetes, just to mention a few.

Prior to the EKG registration the test subject will have to be at rest for 10 min, and is not allowed to have eaten a big meal, smoked or had coffee during a few hours before the event.

Nasal lavage

A salt solution is inserted in the test subject's nose and collected when dripping out. Centrifugation separates the cells and proteins from the solution and the following markers are investigated:

Albumin: the most abundant blood plasma protein. Welders with respiratory problems have been noticed to have elevated levels of this protein, which could be an indicator of plasma excretion and inflammatory activity.

ECP: Eosinophil cationic protein. Eosinophiles (also called acidophiles) are white blood cells that, if activated by an immune stimulus, can release several cationic proteins of which ECP is one. The level of activation in these proteins is a measurement of inflammatory levels.

LDH: Lactate Dehydrogenase (LDH) is an enzyme which is often used as a marker of tissue breakdown since LDH is abundant in red blood cells.

ICAM-1: (Inter-Cellular Adhesion Molecule 1) are proteins that recruits white blood cells from the blood to infected tissue.

Substance P: A neuropeptide that functions as a neurotransmitter and is associated with stress and pain as a part of an inflammatory process.

Fatty acid amides: can be involved in airway inflammations.

Cytokines: A category of signaling molecules that, if in excess, are markers of allergic reactions.

Blood count: The leukocytes (white blood cells) are counted. These are cells of the immune system defending the body against infectious disease and foreign materials.

Rhinometry

Investigates swelling in the nose mucous membrane.

Spirometry

Investigates the lung function by measuring both exhaled volume and exhalation speed.

Blood samples

Fibrinogen: a soluble plasma glycoprotein. Increased levels can indicate a tendency of blood clotting. Excessive generation leads to thrombosis while ineffective generation predisposes to hemorage.

CRP: C-reactive protein is a plasma protein produced by the liver. It is an inflammatory marker.

Cytokines: A cathhegory of signaling molecules that, if in excess, are markers of allergic reactions.

Oxidated proteins: A newly developed method to check for oxidative stress, which is an imbalance involved in many diseases.

RNA: The ribonucleic acid is checked for any genetic impact of the exposure.

Hb: Hemoglobin count.

Exhaled Breath Condensate

The test person exhales into an R-tube, and by studying biomarkers in the exhaled breath airway chemistry and inflammation in the lungs can be investigated (Walsh et al.).

PEF

Peak Expiratory Flow monitors a person's ability to move air by measuring airflow through the bronchi and thus the degree of obstruction in the airways.

RESPI

The main principle of this deposition measurement instrument is to compare the inhaled air with the exhaled. The instrument has been developed by Jakob Löndahl et al at the Division of Nuclear Physics and the Division of Aerosol Technology at Lund University. The fraction of particles deposited in the human lung, DF_{human}, is measured through comparison of the particle concentration as a function of dry size between inhaled (C_{in}) and exhaled (C_{ex}) air, with correction for particle deposition in the instrument (DF_{equip}) according to

$$DF_{human} = 1 - \frac{C_{ex}}{C_{in}(1 - DF_{exuip})}$$

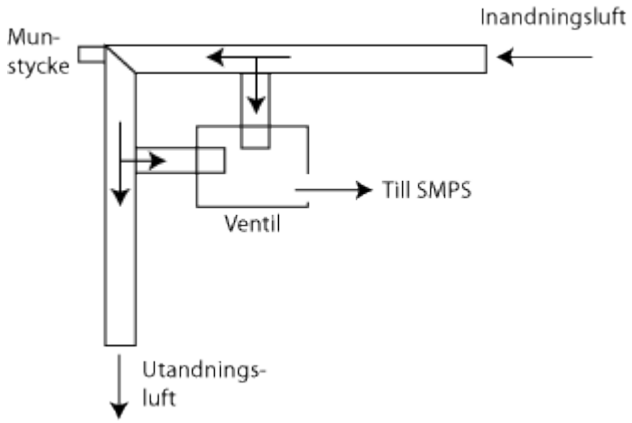

Figure C1. Simplified view of the RESPI system.

The inhaled air originates from the exposure chamber. The exhaled air is directed by two one-way valves into a 2 dm^3 tank that is heated to 33-45 ^oC to prevent condensation. The size of the tank is chosen to minimize both the residens time (and thereby the coagulation) and the concentration gradients within single breaths. The valves are covered with a thin layer of gold to minimize losses by electrostatic deposition. The exhaled air is dried before its size distribution is determined with a scanning mobility particle sizer (SMPS). The software records and simulates the breathing pattern of the human test subject, controls the valves, runs the SMPS and continuously calculates the deposition in the respiratory tract. Flows, temperature and RH are measured by sensors. Every other scan is being made on the exhaled air and every other on the inhaled air (Löndahl et al. 2007)
Previous RESPI measurements have shown that the respiratory tract deposition of candle smoke particles is 60-85 % of the inhaled number concentration, 40-60 % of the inhaled surface concentration and 30-50 % of the mass concentration.

Appendix D

Does an air purifier contribute to the particle removal in the exposure chamber while the express fan is on?

The question is whether a commercial air purifier placed inside the exposure chamber will help to make the air acceptably particle free during the time the express fan is on. This period of time is 15-17 minutes.
Different types of commercial air purifiers are available at the market. They can basically be placed in either of two main categories: the type that removes particles by ionizing the air (*ionic air purifiers*) and the type that removes particles by filtering the air, mainly through HEPA (High Efficiency Particulate Air) filters.

An ionic air purifier uses uni- or bipolar chargers to ionize air molecules thus making particles become charged upon collisions with these molecules. The particles hence migrate to and deposit on surfaces in the room, mainly in the vicinity of the purifier (Grinsphun et al, 2005), which mean that this kind of purifier would contaminate the surfaces of the exposure chamber and should not be considered an alternative for our purposes. A sub category of ionic air purifiers are the *electrostatic precipitators*, which instead makes the particles deposit on collection plates inside the air purifier device. However can the high electrical fields used generate ozone and NO_x – levels as high as 0.05 ppm ozone are being mentioned.

The second category of air purifiers, the ones that uses filtration, are the only type that could come in question for our purposes.
Experiments have been made (Hacker and Sparrow, 2005) by placing several air purifiers (both electrostatic precipitators and the ones that uses HEPA filters) for 8 h in a 31 m^2 chamber, both without ventilation and with an air exchange rate of 4 h^{-1}. Without ventilation (AER = 0) figure D1 shows how the particle concentration decrease without a HEPA air purifier and with one on its maximum effect, respectively.

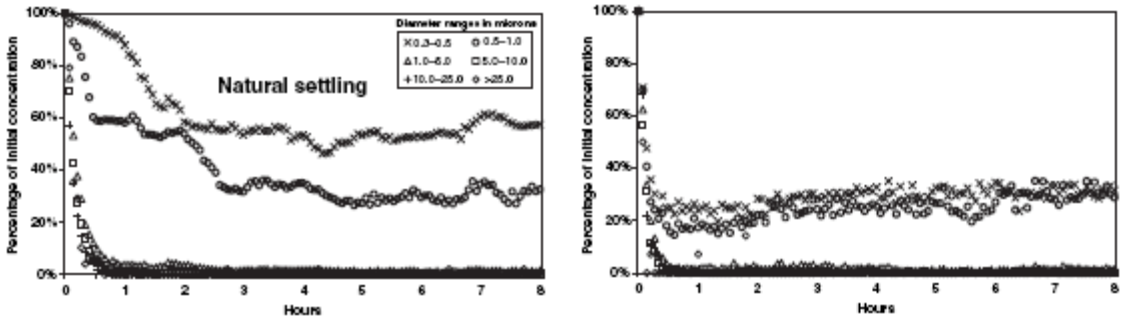

Figure D1. Particle concentration decrease in experiment chamber without and with a HEPA filter air purifier.

Studying the first 15 minutes in the two graphs above makes it apparent that the concentration of the smaller particle fractions decrease to less than half of their initial

levels as an effect of the air purifier. The larger particle fractions are not affected that much since they will have time to sediment (Hacker and Sparrow, 2005).
With an air exchange rate of 4 h^{-1} the situation is as shown in figure D2:

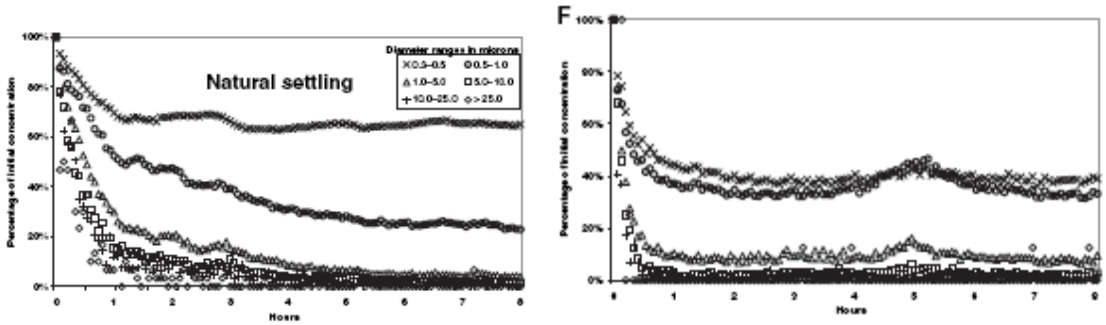

Figure D2. Same situation as in figure D1, but with an AER = 4 h^{-1}.

The flows that arise in the air volume due to the ventilation make the time needed for larger particles to sediment longer. The air cleaner is less effective at these conditions.
Figure D3 shows how the concentration decrease of four different size fractions during a test with candles 070828. Note that the biggest of these size fractions (100 nm) is smaller than the smallest size fraction (300-500 nm) in figure D1 and D2.

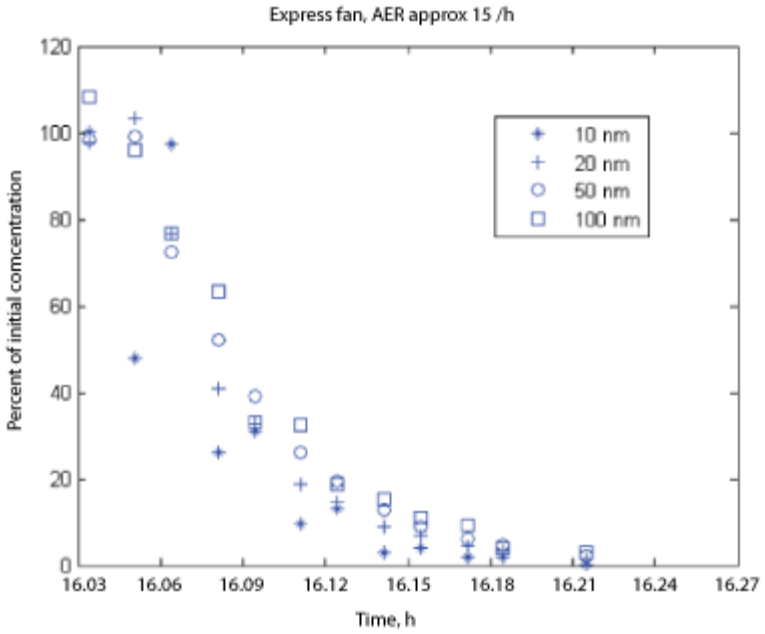

Figure D3. Particles generated by candles. The express fan was on between 10.03 and 16.20. "Initial concentration" means the concentrations of each particle fraction at the time the candles were extinguished and just prior to starting the express fan.

Figure D1 and D2 shows that an air purifier is most effective when no ventilation is on. This theory is also supported by Ward et al. (2005): "…the overall effectiveness of an air-cleaner decreases as the room ventilation increases…".

Figure D3 shows that the express fan is very effective, at least for particle sizes up to 100 nm. In the planned exposure studies particles will be generated by candles, welding fume

and ozone-terpene reactions, neither will generate particles much larger than a few hundred nm (Rohr et al. 2003, Jenkins et al. 2005, Löndahl et al).
Considering the effectiveness of the express fan it can be concluded that an air purifier in combination with this fan will not make the air more particle free than without it, thus we do not need to invest money or energy into this matter.

Appendix E

Particles from VOC-O_3 reactions

Background

Terpenes are a large class of hydrocarbons built by units of isoprene, C_5H_8 (figure E1), so the basic molecular formulas of terpenes are $(C_5H_8)_n$. This is called the *isoprene rule*, or the *C5-rule* (Wikipedia, 2007).

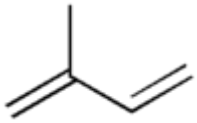

Figure E1. The isoprene unit.

The isoprene units can be linked together in linear chains or to cyclical shapes. As the chains of isoprene units are built up the resulting terpenes are classified according to: Hemiterpenes (one single isoprene unit, hence isoprene itself can be considered to be the only hemiterpene, but oxygene-containing derivates are also hemiterpenoids), Monoterpenes (consists of two isoprene units), Sesquiterpenes[8] (consists of three isoprene units), Diterpenes (consists of four isoprene units), Sesterterpenes[9] (consists of five isoprene units), Triterpenes (consists of six isoprene units), Tetraterpenes (consists of eight isoprene units) and Polyterpenes (consists of long chains of many isoprene units).
When terpenes are chemically modified, through oxidation or through rearrangement of their chain of carbon atoms, the resulting species are called terpenoids. In nature, terpenes are mianly produced by plants, e g pine.
Terpenes can react with ozone in the air and form particles. Limonene, pinene (figure E2) and other ozone reactive terpenes are constituents of many commercial detergents, and they can result in particle mass concentrations in the magnitude of mg/m^3 in indoor air and levels up to tenths- to hundreds of $\mu g/m^3$ can be maintained for several hours after a cleaning event (Singer et al. 2006).

[8] The sesqui-prefix means one and a half.

[9] The sester-prefix means half to three, i e two and a half.

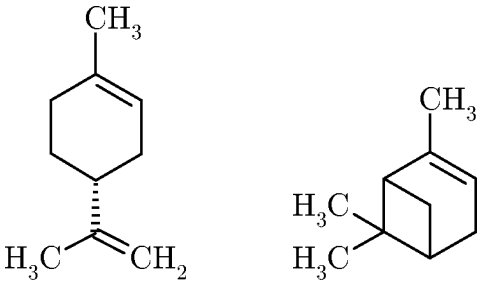

Figure E2. d-limonen and α-pinen. Both are monoterpenes with the chemical formula $C_{10}H_{16}$, α-pinen is bicyclic.

Indoors, the reaction rate between the terpene in question and ozone must be faster than the air exchange rate (AER) for particles to form. Many of the oxidation products in the ozone reaction have low vapor pressure and are therefore capable of self-nucleation or they can condensate onto already existing particulate matter. Ultra fine particles (<0.1 μm) can be formed by homogenous nucleation of the reaction products (Rohr et al. 2003). The condensed phase products tend to contain carbonyl, carboxyl or hydroxyl functional groups. Such groups are hydrophilic and are thus more able to dissolve in mucous in the respiratory tract (Rohr et al. 2003).
Adsorption of reactive terpenoids on surfaces in the home environment prevents them from being removed by ventilation and hence prolongs the time under which they are available for reaction with O_3.
There have also been raports that reactions between certain VOC:s, such as bornylacetate, and the OH radical can generate organic particular matter (Liu et al. 2004).

The level of ozone in the air does not have a substantial impact on the amount of already existing airborne particles, since

1. the reaction of most aerosol constituents with O_3 occurs at rates that are too slow in comparison with the AER
2. collisions between O_3 and aerosol particles occurs much more seldom than collisions between O_3 and VOC or inorganic gases
3. since a particle consists of milions of molecules it literaly takes milions of reactions between O_3-molecules and a particle before the chemistry of the particle is altered (Weschler C. J., 2000).

Indoor concentrations of d-limonene are normally about 0.05-13 ppb and of α-pinene 0.1-21 ppb. During cleaning, top concentrations of more than 550 ppb will normally be reached (the ”smell threshold” for pinene and limonene are 700 and 449 ppb, respectively). (Rohr et al. 2003).
Average indoor ozone concentrations are 28-60 ppb (Rohr et al. 2003), the levels can fluctuate fast, though, it is not unusual that the concentration can change 30-40 ppb within an hour (Weschler 2000). In polluted urban areas the ozone levels can reach 120 ppb during the summer (Singer et al. 2006). Under normal circumstances, the half life of indoor ozone is between 7 and 10 minutes, mainly governed by the surface deposition and the AER (Weschler 2000).
The density of organic aerosols is estimated to be about 1.2 g/cm^3.

Experimental results

Rohr et al. (2003) have made experiments with pure α-pinene and d-limonene while the O_3-koncentration was varied, achieving the following results:
The number concentration at steady state[10] in the α-pinene system was 8.68 $*10^3$ – 1.38$*10^7$ #/cm^3, the masskoncentration 8-14.492 μg/m^3, and for the d-limonene system: 4.96$*10^5$ – 1.65$*10^7$ #/cm^3 and 41-11.213 μg/m^3 respectively. Fewer, but larger particles were obtained for a given concentration of ozone at lower AER, which was expected since a low AER provides longer time for the particles to condensate. The levels of terpenes used for this experiment exceeds normal top indoor values by a factor of 100-1000, the levels of ozone, as well, were considerably higher than the levels in normal indoor air. CMD for the limonene system was 56-115 nm and for the pinene system 45-107 nm. MMD was higher in this system; 170 nm, which indicates that the system is dominated by small particles. There was no obvious impact by the relative humidity on the particle formation in these experiments.Singer et al (2006) shows, though, that the deposition and the decay of ozone increases with increased RH. Products of the O_3 and α-pinen reaction are pinonaldehyd, norpinonaldehyd, pinonic acid and C 10 hydroxydikarbonyler. An O_3/d-limonene system results in limononic acid, 7-hydroxylimononic acid and 7-hydroxy-keto-limononic acid. 22 % of the reaction products in the O_3 / d-limonene system are aerosoles (Weschler 2000).

Singer et al. (2006) have in an experiment used a commercial detergent (pine-oil based general purpose cleaner, POC) in a ”normal” household cleaning way in a wall papered chamber. The AER was 1.0 h^{-1} and the ozone concentration was approximately 120 ppb. The cleaning procedure generated top levels of 170-200 ppb d-limonene, 70-200 ppb terpinolene and 110-130 ppb α-terpineol. The $PM_{1.1}$-concentartion had a peak at about 135 μg/m^3.
Liu et al. (2004) used a stainless steel chamber, 29.8 m^3, in which *air freshener* emissions were allowed to react with O_3. On the basis of these experimental data an existing model (SCIENTIST) was evaluated. The AER was monitored with sulphurhexafluoride (SF_6).
Singer et al. (2006) used, among other things, a detergent of the type that shall be diluted with water prior to use. This was applicated onto different types of surfaces, both with and without wiping the detergent of with water afterwards some of the times leaving the rags behind in the chamber and sometimes removing them directly after use. The detergent generated several different terpenes: α-pinene, camphene, β-pinene, α-phellandrene, α-terpinene, d-limonene, γ-terpinene and terpinolene. The content of terpinolene was about as high as the content of d-limonene, terpinolene, though, has a reaction rate with ozone that is one order of magnitude higher than that for d-limonene. α-terpinen reacts two orders of magnitude faster with ozone than d-limonene, but the content of α-terpinen was only 1/10 of that of d-limonene.

[10] Steady state is the point in time at which, within a given particle size, the processes populating the size range match those depopulating the size range. Steady state thus occurs in the chamber after an “equilibrium” is reached between gas-to-particle conversion (i e nucleation, condensation) as well as particle growth processes.

Methods for generation of VOC and O_3

O_3 can be generated by letting dry 100 % O_2 pass through UV-light (Rohr et al. 2003). When a molecule of oxygene, O_2, is exposed to light of the wavelength 240 nm it decays to two oxygene atoms. One such atom will in turn react with an oxygene molecule to form ozone. It is also possible to use a *high frequency corona discharge O_3 generator* (*OzoneLab* GE30/FM100R) (Singer et al. 2006), Singer et al introduced the ozone to the chamber at least 12 hours prior to conducting the experiments.

The methods for VOC generation are, of course, dependent on weather one wishes to obtain pure terpenes or use commercial detergents. Fume of pure terpenes can be generated by allowing compressed nitrogen pass through a bottle of terpene solution (Rohr et al. 2003) and then dilute this flow with particle free air. The aim is to let the concentration of terpenes to exceed the concentration of O_3 so that the reaction becomes ozone-limited, since the levels of ozone indoors does not vary in the same way the terpene levels does. Singer et al. (2006) genererated VOC by in a very well-controlled manner clean the floor of the exposure chamber with detergent diluted with water according to the proportions stated on the bottle.

Methods for measurments

An UV ozone detektor is often used for measuring O_3, VOC can be monitored with GC-MS, in some cases combined with FID, and the resulting aerosol with teflone filters and SMPS.

To estimate the emissions of VOC from one ”cleaning event” Singer et al. (2006) employed a method for, with the help of a material balance, calculating effective emissionfactors (milligrams of constituent emitted per gram of total detergent product used). The basic assumption for these calculations is that the effective net mass emitted to the air is finally balanced by the mass that is removed from the chamber through ventilation. In a well mixed chamber the removal rate is decided by the time integral of product concentration ($\mu g/m^3$) in the chamber air (background concentrations corrected for) multiplied by the ventilation rate (m^3/min). The emission factors are termed “effective” since they reflects the net result of partly the ground emission (from applying the detergent) and partly the emission contribution from the towels or rags used, desorption from the cleaned surfaces and the adsorption onto other surfaces in the chamber. The emission factors can then be multiplied by the application amount (g/m^2) and by the application area (m^2), which render an estimation of how much VOC the cleaning procedure in question have generated. Since the emission factors gives the mass of the different analytes measured in the air, they are relevant for estimations of the inhalation exposure. The emission factors vary strongly depending on which cleaning method is being employed.

Further work

When Ebersviller et al. made an experiment using two identical chambers with identically high flows of ozone (10 ppb/min) and using equal amounts of d-limonene, though it in one of the chambers was added in its pure form and in the other chamber in the form of a detegent product, they obtained an obvious difference between the two chambers, both in the gas and in the particle phase. Since there obviously is a difference in both oxidation products as well as in the amount of obtained particles, the relevance of using pure terpene as a substitute for detergent when examining particle formation can be questioned. Using a real, commercial detergent also provides a real life relevance which makes the study of health effects more pertinent. Of course, this leaves the researchers with the problems of deciding upon which detergent brand to use, since they can provide somewhat different reaction products resulting in different health effects.

Appendix F

Exposure schedules

Indoors – 3 hours exp

Plan tid 07.30	**Undersökning före exponering**	**Kl**	**Sign**	**Status/kommentar**
	Lämna urinprov 1 + ombyte			
	Symptomfrågor + PEF 1			
	Läkarundersökning 1			
8.10	HRV 1			
8.30	Nässköljning 0			
	Utandningskondensat 1			
	Spirometri 1			
	Rhinometri 1			
	Blodprov 1			
	Nässköljning 1			
9.30	**Start Exponering**			
9.40	Symptomfrågor 2 + PEF – efter 10 min			
10.00	HRV 2			
10.40	Symptomfrågor 3 + PEF – efter 1 tim			
11.00	HRV 3			
11.40	Symptomfrågor 4 + PEF – efter 2 tim + stopp matintag			
12.20	Symptomfrågor 5 + PEF – innan evakuering			
12.30	**Slut Exponering**			
	HRV 4			
12.50	**Ut ur kammare**			
	Läkarundersökning 2			
13.00	Nässköljning 2			
	Utandningskondensat 2			
	Rhinometri 2			
	Spirometri 2			
	Blodprov 2			
	Urinprov 2			

Welding – 5 hours exp

Plan tid 07.30	Undersökning före exponering	Kl	Sign	Status/kommentar
	Lämna urinprov 1 + ombyte			
	Symptomfrågor + PEF 1			
	Läkarundersökning 1			
8.10	HRV 1			
8.30	Nässköljning 0			
	Utandningskondensat 1			
	Spirometri 1			
	Rhinometri 1			
	Blodprov 1			
	Nässköljning 1			
9.30	**Start Exponering**			
9.40	Symptomfrågor 2 + PEF – efter 10 min			
10.00	HRV 2			
10.40	Symptomfrågor 3 + PEF – efter 1 tim			
11.00	HRV 3 + stopp matintag			
11.45	Symptomfrågor 4 + PEF – efter 2.5 tim			
12.00	**Ut ur exponering**			
	Läkarundersökning 2			
	Utandningskondensat 2			
	Lunchuppehåll med RESPI **Fylla i arvodesblankett**			
13.30	Start exponering efter lunch			
13.40	Symptomfrågor 5 + PEF – efter 10 min			
14.00	HRV 4			
14.30	Symptomfrågor 6 + PEF – efter 4 tim			
15.00	HRV 5 + stopp matintag			
	Symptomfrågor 7 + PEF – innan evakuering			
16.00	**Slut exponering**			
	HRV 6			
16.20	**Ut ur kammare**			
	Läkarundersökning 3			
16.30	Rhinometri 3			
	Spirometri 3			
	Blodprov 3			
	Nässköljning 3			
	Utandningskondensat 3			
	Urinprov 3			

Appendix G

Technical specifications for ESAB Aristorod™ 12.50

Classifications	Approvals		Typical all weld metal composition, %		Typical mech. properties all weld metal	
SFA/AWS A5.18	ABS	3SA, 3YSA	C	0,1	Yield stress, MPa	
ER70S-6			Si	0,9	470	
EN 440	BV	SA3YM	Mn	1,5	Tensile strength, MPa	
G3Si1	CWB	CSA W48	Wire composition		560	
	DB	42.039.29			Elongation, %	
	DNV	III YMS			26	
	DS	EN 440			Elongation, %	
	GL	3YS			26	
	LR	3S, 3YS			Charpy V	
	VdTÜV				Test temps, °C	Impact values, J
					+20	130
					-20	90
					-30	70

Diameter, mm	0,8	0,9	1,0	1,2	1,4	1,6
Arc voltage, V	18-24	18-26	18-32	18-35	22-36	28-38
Welding current, A	60-200	70-250	80-300	120-380	150-420	225-550
H. Kg weld metal/hour arc time		-	-	-	-	-
Wire feed, m/min	3,2-10	3,0-12	2,7-15	2,5-15	2,3-12	2,3-15
Deposition rate kg weld metal/hour	0,8-2,5	0,8-3,3	1,0-5,5	1,3-8,0	1,6-8,7	2,1-11,4